

UC Berkeley

UC Berkeley Previously Published Works

Title

Multilevel analysis between *Physcomitrium patens* and Mortierellaceae endophytes explores potential long-standing interaction among land plants and fungi

Permalink

<https://escholarship.org/uc/item/7wt66671>

Journal

The Plant Journal, 118(2)

ISSN

0960-7412

Authors

Mathieu, Davis
Bryson, Abigail E
Hamberger, Britta
[et al.](#)

Publication Date

2024-04-01

DOI


10.1111/tpj.16605

Copyright Information

This work is made available under the terms of a Creative Commons Attribution License, available at <https://creativecommons.org/licenses/by/4.0/>

Peer reviewed

Multilevel analysis between *Physcomitrium patens* and Mortierellaceae endophytes explores potential long-standing interaction among land plants and fungi

Davis Mathieu^{1,2}, Abigail E. Bryson^{1,2}, Britta Hamberger², Vasanth Singan³, Keykhosrow Keymanesh³, Mei Wang³, Kerrie Barry³, Stephen Mondo^{3,4,5}, Jasmyn Pangilinan³, Maxim Koriabine³, Igor V. Grigoriev^{3,6}, Gregory Bonito^{1,7} and Björn Hamberger^{1,2,*} 

¹Genetics and Genome Science Graduate Program, Michigan State University, East Lansing, Michigan, USA,

²Department of Biochemistry and Molecular Biology, Michigan State University, East Lansing, Michigan, USA,

³U.S. Department of Energy Joint Genome Institute, Lawrence Berkeley National Laboratory, Berkeley, California 94720, USA,

⁴Department of Agricultural Biology, Colorado State University, Fort Collins, Colorado 80523, USA,

⁵Environmental Genomics and Systems Biology Division, Lawrence Berkeley National Laboratory, Berkeley, California 94720, USA,

⁶Department of Plant and Microbial Biology, University of California Berkeley, Berkeley, California 94720, USA, and

⁷Department of Plant, Soil and Microbial Sciences, Michigan State University, East Lansing, Michigan, USA

Received 4 August 2023; revised 16 November 2023; accepted 13 December 2023.

*For correspondence (e-mail hamberge@msu.edu).

SUMMARY

The model moss species *Physcomitrium patens* has long been used for studying divergence of land plants spanning from bryophytes to angiosperms. In addition to its phylogenetic relationships, the limited number of differential tissues, and comparable morphology to the earliest embryophytes provide a system to represent basic plant architecture. Based on plant–fungal interactions today, it is hypothesized these kingdoms have a long-standing relationship, predating plant terrestrialization. Mortierellaceae have origins diverging from other land fungi paralleling bryophyte divergence, are related to arbuscular mycorrhizal fungi but are free-living, observed to interact with plants, and can be found in moss microbiomes globally. Due to their parallel origins, we assess here how two Mortierellaceae species, *Linnemannia elongata* and *Benniella erionia*, interact with *P. patens* in coculture. We also assess how *Mollicute*-related or *Burkholderia*-related endobacterial symbionts (MRE or BRE) of these fungi impact plant response. Coculture interactions are investigated through high-throughput phenomics, microscopy, RNA-sequencing, differential expression profiling, gene ontology enrichment, and comparisons among 99 other *P. patens* transcriptomic studies. Here we present new high-throughput approaches for measuring *P. patens* growth, identify novel expression of over 800 genes that are not expressed on traditional agar media, identify subtle interactions between *P. patens* and Mortierellaceae, and observe changes to plant–fungal interactions dependent on whether MRE or BRE are present. Our study provides insights into how plants and fungal partners may have interacted based on their communications observed today as well as identifying *L. elongata* and *B. erionia* as modern fungal endophytes with *P. patens*.

Keywords: *Physcomitrium patens*, Mortierellaceae, differential expression, gene ontology enrichment, RaspberryPi, PlantCV.

INTRODUCTION

Plants and fungi have a long history of symbiosis and cohabitation, with over 90% of modern land plants demonstrating some degree of mutualism (Bonfante & Genre, 2010; Smith & Read, 2010). In addition to the high frequency of plant–fungal interaction among land plants, the

observed mutualism extending to algae and lichens implies that the emergence of traits allowing for a beneficial exchange of compounds between plant and fungus arose even earlier in chlorophyllic phototroph evolution (Du et al., 2019; Duckett et al., 2006; Hanke & Rensing, 2010; Knack et al., 2015; Kohler et al., 2015; Liepina, 2012; Loron

et al., 2019; Lutzoni et al., 2001, 2018; Morris et al., 2018; Nelsen et al., 2020; Russell & Bulman, 2005). Although bacteria and fungi are known to have dominated the terrestrial landscape long before plant terrestrialization, the ability of plant and fungal kingdoms to interact early in embryophyte evolution may have enabled the global takeover of both Kingdoms. Today, this relationship is exemplified through plants exchanging a reliable carbon source via the products of photosynthesis (i.e., sugars and fatty acids) and nearly ubiquitous symbiosis with filamentous fungi that exchange nitrogen, phosphorous, micronutrients, metabolites, and water retention (Bonfante & Genre, 2010; Martin & Nehls, 2009). Further, modern plant and fungal symbionts have been shown to mitigate many shared stresses such as oxidative, osmotic, heat, UV radiation, and rapid temperature flux (de Vries & Archibald, 2018; Du et al., 2019; Fürst-Jansen et al., 2020; Jermy, 2011; Kohler et al., 2015; Lutzoni et al., 2018). These same stresses would have posed significant barriers to entry for the first terrestrial land plants as well. The early emergence of plant–fungal interactions may have reduced constraints imposed by the ancient terrestrial landscape and consequently may have led to the global expansion of plants and fungi observed today.

While many plant–fungal mutualists have been identified in embryophytes, no reports of fungal mutualism in the model moss *Physcomitrium patens* (formerly *Physcomitrella patens*) have been made (Bonfante & Genre, 2010; Read et al., 2000). This is despite many arbuscular mycorrhizal fungi that have demonstrated a capacity for mutualism in other bryophytes like hornworts and liverworts (Fonseca & Berbara, 2008; Ligrone et al., 2007). *P. patens* is capable of specialized fungal response although this is largely in the context of combatting parasitic fungi which otherwise would decrease host fitness (Bressendorff et al., 2016; Davey et al., 2009; Delaux & Schornack, 2021; Lehtonen et al., 2009, 2012; Mittag et al., 2015; Ponce de León, 2011; Ponce De León et al., 2012). Additionally, evidence that *P. patens* has (or had) the capacity for interacting with fungi can be supported by the presence of orthologs essential to detecting and forming plant–fungal interaction. Some conserved genes that are indicative of this possibility include a chitin-like receptor *PpCERK1* necessary to signal the environmental presence of fungi, a *VAPYRIN*-like homolog with only known function in forming symbiotic interaction between plants and fungi, and functional strigolactone hormone pathways with secondary functions known to signal host root proximity to symbiotic and parasitic fungi (Bressendorff et al., 2016; Delaux & Schornack, 2021; Proust et al., 2011; Rathgeb et al., 2020).

Here we investigate two filamentous fungal species belonging to Mortierellaceae as potential symbiotic candidates with *P. patens*. Mortierellaceae are a lineage of free-

living fungi closely related to arbuscular mycorrhizal fungi, that are known to improve aboveground plant growth and development and to associate with plants as endophytes (Vandepol et al., 2022; Johnson et al., 2019; Zhang et al., 2020). Fungi in Mortierellaceae embody many promising traits as a mutualist, sharing an evolutionary history with the widespread but host-dependent arbuscular mycorrhizal fungi (AMF) and forming mutualisms with chlorophytes (algae), *Arabidopsis thaliana*, and other embryophytes (Becker & Cubeta, 2020; Du et al., 2019; Johnson et al., 2019; Liao et al., 2021; Rensing et al., 2008; Vandepol et al., 2022; Zhang et al., 2020). Interestingly, species in both AMF and Mortierellaceae can be colonized by either Mollicute-related endobacteria (MRE) or Burkholderia-related endobacteria (BRE), which grow within host cells and are nutritionally dependent on the host. We investigated interactions of *P. patens* with *Linnemannia elongata* (formerly *Mortierella elongata* strain NVP64) and *Benniella erionia* (formerly strain GB_Aus27b), either carrying (WT) or cleared (CU) of its bacterial endosymbiont (described in more detail below). There are multiple reports of *L. elongata* forming mutualistic interactions with algae and plants in ways that increase plastid size, aboveground plant growth, flowering, and seed production in different plant species (Du et al., 2019; Liao et al., 2021; Vandepol et al., 2022). In contrast, the recently described fast-growing fungus *B. erionia* caused chlorosis in interactions with the algal species *Nannochloropsis oceanica* and *Chlamydomonas reinhardtii* (Du et al., 2019). The lack of identified interaction of *P. patens* with AMF, which is the most widespread embryophytic mutualist seen today (Feijen et al., 2018), may be due to AMF predominantly colonizing roots, a tissue absent in moss. Despite the current global abundance of AMF, ancestral reconstruction suggests that the prolificity seen today parallels the emergence and expansion of angiosperms 250 MYA, while the fungal species detected during plant terrestrialization more closely resembles Mortierellaceae (Feijen et al., 2018).

We also assessed the impact of endobacterial symbionts of fungi on fungal–moss interactions. Previous studies have shown that MRE and BRE intracellular bacteria can be removed from the hosts with antibiotics, which results in changed fungal growth and metabolism (Desirò et al., 2018; Uehling et al., 2017; Vandepol et al., 2022). As *L. elongata* naturally contains BRE and *B. erionia* naturally contains MRE, we carried out our experiment using isogenic isolates either with (WT) or without (CU) endosymbionts. Previous studies with AMF have found that BRE increases sporulation in their host and improves energy capacity/availability, often at the expense of a reduced growth rate (Alabid et al., 2019; Salvioli et al., 2016; Uehling et al., 2017). While the impact that endobacteria have on *L. elongata*, *B. erionia*, and their fungal–plant interactions are unclear, endobacteria are known to influence

how fungi interact with their environment and therefore may play an important role in plant–fungal interactions (Desirò et al., 2018; Guo & Narisawa, 2018; Ohshima et al., 2016; Uehling et al., 2017; Vandepol et al., 2022).

To measure the interaction between fungal endophytes and *P. patens*, we investigated the interaction at organismal, cellular, and transcriptional levels. This was accomplished through a custom built phenomics platform and analysis pipeline, brightfield microscopy, and RNA sequencing with subsequent expression analysis. Broader influences were also investigated through the incorporation of transcriptional analysis data and comparison with the results from the 'Physcomitrella patens Gene Atlas Project' ('Gene Atlas Project'), which examined 99 RNA-seq expression datasets generated in *P. patens* (Perroud et al., 2018). Our results indicate distinct responses in *P. patens* when cocultured with *B. erionia* or *L. elongata* and the nature of their response being dictated by endobacteria. Here, we propose that *P. patens* has retained some ability to interact with Mortierellaceae endophytically based on the observation of asymptomatic intracellular colonization of fungi within plant tissues and these colonizations potentially being dependent upon the presence of endobacteria. These observations provide insights into an interaction that may have originated 500 MYA (Feijen et al., 2018; Hobbie & Boyce, 2010; Ivarsson et al., 2020).

RESULTS AND DISCUSSION

Development and implementation of high-throughput phenomics approach monitors *P. patens* growth

We have created and utilized a novel phenomics platform which can automatically capture *P. patens* growth over time with exceptional sensitivity and throughput. Over the course of 2 months and 40 samples, we generated over 2000 time-stamped images. These images were quantified with resolution indicating growth changes at the millimeter scale (Data S1a,b). This was accomplished by using RaspberryPi for image capture and the software PlantCV to quantify plant growth. While sample germination differed between replicates, no systematic advantage or penalty to health was observed for either *P. patens* or fungal partners. Hence, the results at the scale and macroscopic resolution of this experiment do not generate decisive results regarding either negative or positive effects on growth (Figure 1). This phenomics approach also provided additional benefits in confirming the cohabitation of both species throughout the entirety of the growth period (Data S1a).

Microscopy reveals *P. patens* responds differently and uniquely to each fungal strain

To investigate the physical interaction of fungal species with *P. patens* at a cellular resolution, combinations were subjected to histology. Fungal hyphae were often

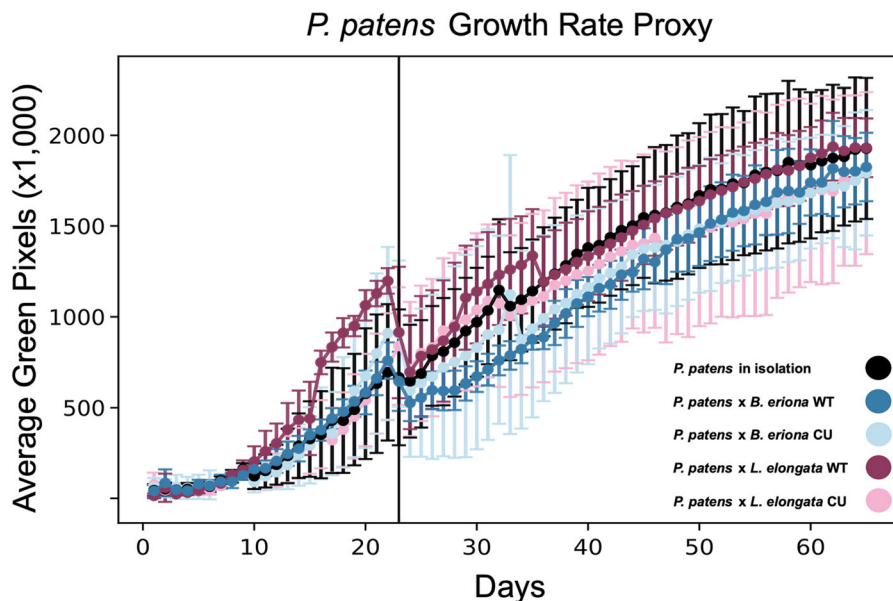


Figure 1. Daily quantified growth of *Physcomitrium patens* over 65 days compared to samples inoculated with either *Bennettia erionia* WT, *B. erionia* CU, *Linne-mannia elongata* WT, or *L. elongata* CU.

Average daily green pixel count with standard deviation of *P. patens* grown in isolation (black) or grown in coculture with *B. erionia* WT (dark blue), *B. erionia* CU (light blue), *L. elongata* WT (magenta), *L. elongata* CU (pink). All samples grew without fungi until day of inoculation (Day 23) indicated by vertical black line, in which fungal inoculated (or uninoculated) perlite were added to their respective samples predetermined by a random number generator. The dip in growth on the day of inoculation can be attributed to perlite covering up already-grown moss tissue.

© 2024 The Authors.

The Plant Journal published by Society for Experimental Biology and John Wiley & Sons Ltd.,
The Plant Journal, (2024), doi: 10.1111/tpj.16605

identified near or within ruptured plant cells, suggesting all fungal samples may have saprotrophic tendencies. Complementing our phenomic observations, all cocultures showed successful cohabitation with clear maturation and growth of both plant and fungi on BCD agar. *B. erionia* WT cocultures had the most common occurrences of fungal hyphae inhabiting ruptured *P. patens* cells and the highest abundance of hyphae within plant cells. Additionally, we found multiple characteristic instances of *B. erionia* WT hyphae inside *P. patens* where the plant cell had also retained turgor pressure (Figure 2a). Representative colonized cells experienced bleaching and lacked any observable chloroplasts, with neighboring *P. patens* cells containing an abnormally high density of chloroplasts (Figure 2a). Infected *P. patens* cells were typically limited to a single cell without passage through cellular junctions, which could indicate successfully suppressed infection by

P. patens. In contrast, *P. patens* and *B. erionia* CU cocultures showed no visible interaction, indicating the potential relevance of endobacteria for colonization. While the exact function(s) of endobacteria in fungi is still speculative, they appear to confer a higher resiliency to environmental conditions and better fungal germination rate in some cases, with evidence here suggesting in some cases endobacteria may also have an influential role in fungal colonization in plant hosts (Naumann et al., 2010; Salvioli et al., 2016).

Linnemannia elongata WT cocultures also exhibited intracellular colonization, however, *P. patens* retained cellular chloroplast content within fungal inhabited cells (Figure 2b,c). Unlike *B. erionia* WT, *L. elongata* WT hyphae were observed to cross *P. patens* cellular junctions (Figure 2c). The retention of chloroplasts, the spread of intracellular hyphae, and the retention of turgor pressure in *P. patens* with *L. elongata* WT indicate a less intrusive

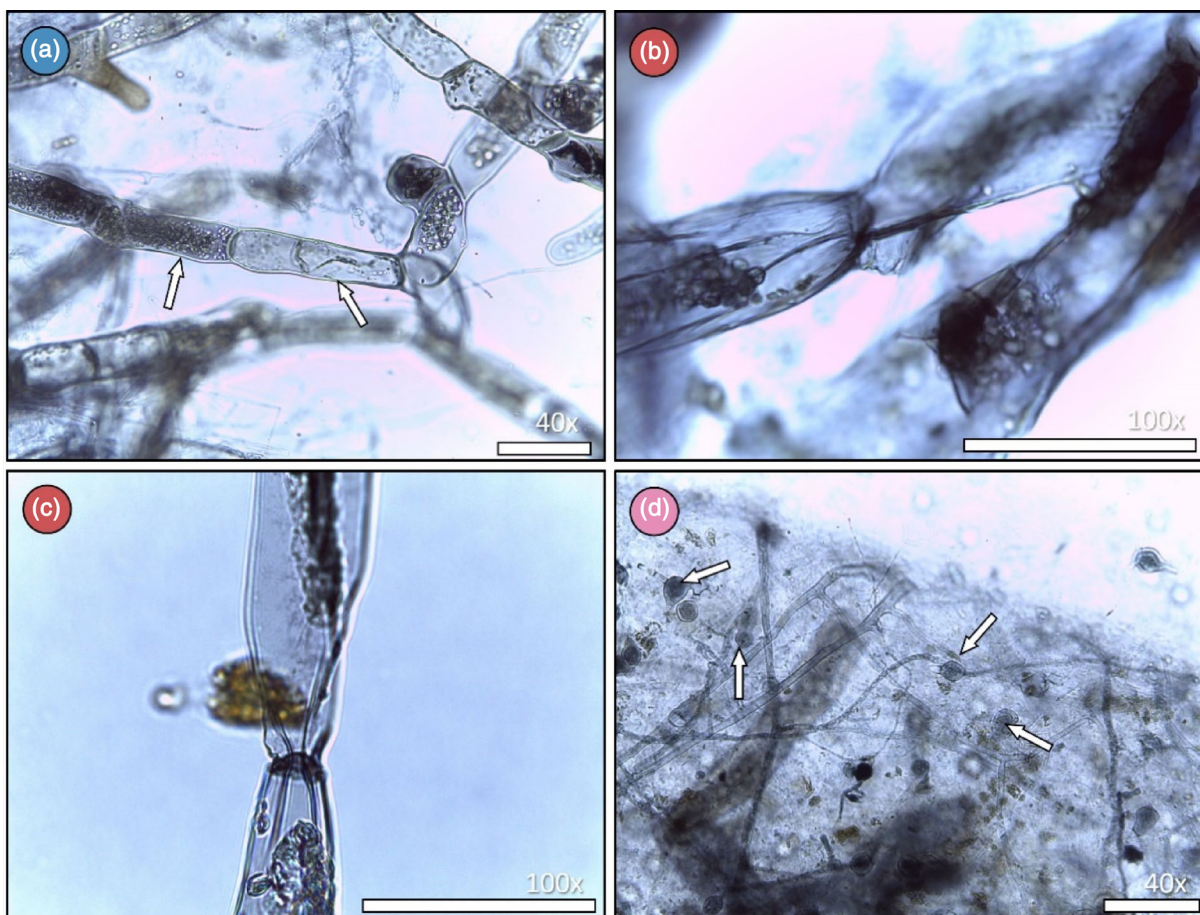


Figure 2. Representative and specific interaction of *Physcomitrium patens* with *Benniella erionia* and *Linnemannia elongata* (White bar indicates 50 μ m for each picture).

- (a) Two unruptured *P. patens* protonema cells, one of which (right arrow) has experienced major chlorosis and appears to have a *B. erionia* hyphae encapsulated within the cell, while the neighboring *P. patens* cell (left arrow) has an abnormally high abundance of chloroplasts.
 (b) *L. elongata* WT hyphae spanning intercellularly between two *P. patens* cells.
 (c) Second occurrence of *L. elongata* WT colonizing *P. patens* cells with *L. elongata* WT bridging the gap between *P. patens* cellular junction points.
 (d) Abundance of *L. elongata* CU sporing bodies in cell culture.

interaction. *L. elongata* CU uniquely inhabits its environment compared to all other samples by producing a high abundance of chlamydo spores (Figure 2d) (Nguyen et al., 2019). Because of this unique environmental colonization, it is possible that *L. elongata* CU induces a different and unique *P. patens* response compared to the other fungal cocultures. Based on the lack of colonization of *P. patens* from both cured Mortierellaceae strains and colonization from both WT, it appears that endobacteria may be a critical component for both *L. elongata* and *B. erionia* to interact endophytically.

Comparative transcriptomics indicates distinct response in *P. patens* by *L. elongata*, *B. erionia*, and endobacterial presence

Our study consisted of 15 transcript libraries, containing 5 different treatment groups with 3 replicates each. Among the metadata, mapped reads mainly aligned to the *P. patens* transcriptome ($99.1 \pm 1.2\%$ [95% CI]). The 0.9% of reads to map to a fungal transcriptome were heavily inflated by replicates in *P. patens* × *L. elongata* CU cocultures (CUTPG, CUTPC, and CUTPH), which represented 0.5, 1.7, and 8.4% of total mapped reads respectively. This is in contrast to the other nine fungal coculture samples, which

generally mapped less than 0.01%. The pool of total mapped fungal reads, even with *L. elongata* CU samples, was not sufficiently representative for analysis of transcriptomic response in fungi. Our principal component analysis (PCA) showed that the derived variance between samples led to two major clusters based on transcriptomic response (Figure 3). Consistent with the distinct microscopic interaction observed, cocultures indicating stress responses in *P. patens* (Cluster B: *B. erionia* WT and *L. elongata* CU) clustered separately from samples speculated to induce a neutral response [Cluster A: uninoculated *P. patens*, *B. erionia* CU, and *L. elongata* WT (Figure 3)].

Additionally, investigating the identified gene homologs necessary for plant–fungal symbiosis (Delaux et al., 2015) presents strong differences between WT and CU strains of each fungal species effects on *P. patens* (Data S8). The presence of endobacteria seems to influence the *P. patens* symbiotic genes in these strains inversely, where *B. erionia* CU and *L. elongata* WT have no hits and only 1 DEG (Downregulated GRAS transcription factor) respectively represented in both strains. That contrasts strongly with *B. erionia* WT and *L. elongata* CU with 20 DEGs and 14 DEGs respectively and among those hits, 8 DEGs (1 MLD-Kinase; 2 CDPKs; 5 GRAS transcription

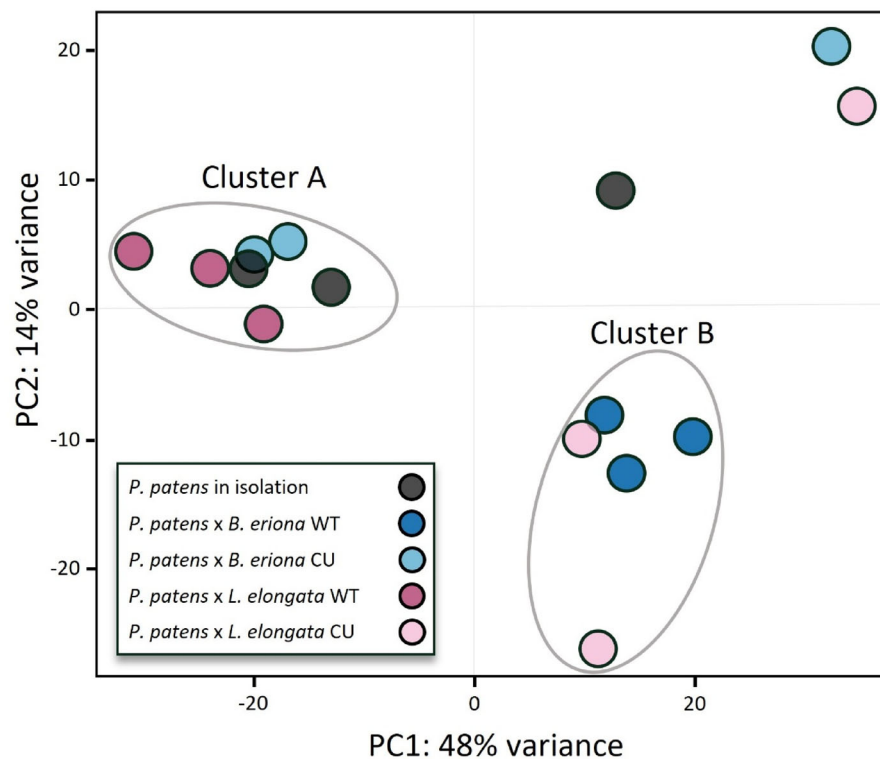


Figure 3. Principal component analysis (PCA) of *Physcomitrium patens* mapped RNA-seq reads for the 15 RNA-sequencing libraries generated with DeSEQ2. The color of each point correlates to experimental treatment. *P. patens* control grown in isolation (black), and *P. patens* treatments grown in coculture with *Benniella erionia* WT (dark blue), *B. erionia* CU (light blue), *L. elongata* WT (magenta), and *L. elongata* CU (pink).

factors) were shared and regulated the same between both strains (Data S8).

Of all the treatments investigated (fungal presence, *B. erionia* coculture, *L. elongata* coculture, and endobacteria presence/absence) we identified that the combined effects from species and endobacteria were the most informative as each induced unique responses in *P. patens*. This phenomenon is especially illustrated by 75.4% of all DEGs being unique to a specific fungal coculture (Figure 4; Data S2a–d).

Transcriptomic response from *B. erionia* WT suggests infectious activity in *P. patens*

Among the four fungal treatments, *P. patens* cocultured with *B. erionia* WT had the most definitive response phenotypically and transcriptomically. There were 2586 total significant differentially expressed genes (DEGs) ($P_{\text{adj}} < 0.01$), with 1533 upregulated and 1053 downregulated (Data S2b). Gene groups with overrepresented expression in *B. erionia* WT cocultures had ontology enrichment, especially with function in transmembrane transport, calcium/inorganic ion transport, and localization (Data S4). Consistent with the observed chloroplast rerouting between colonized plant cells, the enrichment of organelle transport genes supports that *P. patens* transcriptomically responds to contain fungal infection and limit organelle damage by changing cellular organization, which is an observed infection response (Savage et al., 2021). Of specific transporters, a putative syntaxin transporter was

highly represented among *B. erionia* WT coculture gene hits and is shown to function in cellular reorganization for the shuttling/protection of organelles in other systems (Table 1) (Hachez et al., 2014). Ion transport, particularly calcium, was also overrepresented. Calcium channels are essential for cell signaling locally and globally within plant systems, notably influencing immune response for both parasitic and symbiotic fungi (Chen, Gutjahr, et al., 2015; Ivashuta et al., 2005) and also can direct the tethering or relocation of organelles (Allan et al., 2022; Tominaga et al., 2012). Additional transporters from DEGs included a chloroquine resistance transporter, whose homologs have been affiliated with regulating abiotic stress in *Arabidopsis* (Maughan et al., 2010; Waller et al., 2003), as well as a nodulin-like transporter. Nodulin-like transporter homologs have been observed in other non-nodulating systems and play important roles not only in the transport of micronutrients but also are critical for communication between the plant–fungal interface for symbiosis and infection (Akiyama et al., 2005; Besserer et al., 2006; Denancé et al., 2014; Waters et al., 2013).

Pathways influencing photosynthesis, abiotic stimuli response, and transcriptional regulation saw substantial depletion in expression (Data S4). Photosynthesis changed most prominently with 28 related GO terms having decreased expression in coculture, including chlorophyll binding, photosystem I and II, thylakoid activity, and chloroplast activity (Data S4). Photosynthesis pathways play an important role in plant immunity. Reduced photosynthesis

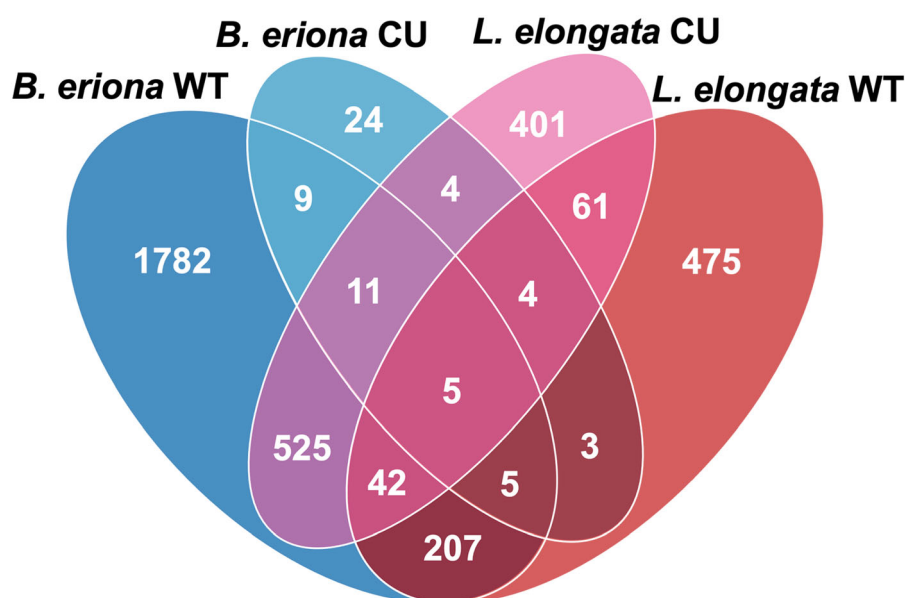


Figure 4. Venn diagram of differentially expressed genes (DEGs) between *Physcomitrium patens* control and *P. patens* co-cultures with *Benniella erionia*, WT (dark blue), *B. erionia* CU (light blue), *L. elongata* WT (red), and *L. elongata* CU (pink).

Total DEGs called by DESeq2 and their significance between each treatment. Genes qualified as differentially expressed if they had expression differences with $P_{\text{adj}} < 0.01$ compared to *P. patens* control.

Table 1 Representative differentially expressed genes from each coculture that exemplify the enriched/depleted ontologies and the unique interactions

Coculture	Ontology	Regulation	Gene(s)	Expression	Annotation	Log ₂	P _{adj}	
<i>B. erionia</i> WT	Transport/localization	Enriched	Pp3c19_4690	↑	Syntaxin transporter	4.23	1.14 × 10 ⁻⁴⁰	
		Enriched	Pp3c16_7270	↑	Membrane protein	2.12	7.01 × 10 ⁻⁴⁰	
		Enriched	Pp3c14_6070	↑	ATP-binding cassette transporter	2.28	3.12 × 10 ⁻³¹	
		Enriched	Pp3c1_4260	↑	Predicted transporter protein	1.77	2.60 × 10 ⁻⁴⁵	
		Enriched	Pp3c9_2960	↑	Nodulin-like transporter	3.08	6.06 × 10 ⁻²⁸	
		Enriched	Pp3c6_18950	↑	Chloroquine resistance transporter	2.69	6.06 × 10 ⁻²⁸	
	Carbon metabolism	n.s.	Pp3c4_25090	↑	Carboxykinase	2.77	4.00 × 10 ⁻⁴⁰	
		n.s.	Pp3c14_11970	↑	Exostosin-related gene	2.07	5.74 × 10 ⁻³⁶	
		n.s.	Pp3c21_16620	↑	Cellulose/cell wall biosynthesis	3.38	2.47 × 10 ⁻³⁶	
		n.s.	Pp3c5_19530	↑	Cellulose/cell wall biosynthesis	1.96	3.17 × 10 ⁻²⁶	
		n.s.	Pp3c1_41400	↑	Cellulose/cell wall biosynthesis	1.72	3.21 × 10 ⁻²²	
		n.s.	Pp3c15_25660	↑	Cellulose/cell wall biosynthesis	1.68	5.85 × 10 ⁻²²	
	Transcription factor	n.s.	Pp3c19_3000	↑	WRKY transcription factor	3.31	3.12 × 10 ⁻³¹	
		n.s.	Pp3c19_8700	↑	Protein TIFY	2.36	3.86 × 10 ⁻³¹	
		n.s.	Pp3c6_2730	↑	HEX transcription factor (leaflet specific)	2.17	4.12 × 10 ⁻²³	
	Isoprenoid synthesis	n.s.	Pp3c1_10000	↑	Hydroxymethylglutaryl-CoA reductase	1.57	2.94 × 10 ⁻³⁰	
	Stress response	n.s.	Pp3c19_17670	↓	BAG family molecular chaperone regulator	-2.22	3.19 × 10 ⁻²⁷	
		n.s.	Pp3c19_10440	↓	DNAJ homolog subfamily	-1.54	1.04 × 10 ⁻²⁵	
	<i>B. erionia</i> CU	Extracellular sensing	Enriched	Pp3c26_13260	↑	Ethylene response transcription factor	1.68	2.80 × 10 ⁻⁴
			Enriched	Pp3c23_11030	↑	MYB-like transcription factor	1.83	4.01 × 10 ⁻⁴
Cell wall response		Enriched	Pp3c4_24020	↑	Cell wall assembly regulator	1.51	9.86 × 10 ⁻⁶	
<i>L. elongata</i> WT	Isoprenoid synthesis	n.s.	Pp3c7_1880	↓	Ent-kaurene synthase	-1.50	1.91 × 10 ⁻⁶	
	Cytoskeletal reorganization	Enriched	Pp3c18_1430	↑	Myosin ATPase	0.90	2.19 × 10 ⁻⁶	
		Enriched	Pp3c5_7180	↑	Chlorophyll A/B binding protein	1.29	3.07 × 10 ⁻¹⁰	
	Cell wall biogenesis/polysaccharide synthesis	Enriched	Pp3c17_5150	↑	Beta-1-3-glucanase	1.45	1.23 × 10 ⁻⁷	
		Enriched	Pp3c3_20980	↑	GDP-fucose transferase	0.90	5.11 × 10 ⁻⁶	
		Enriched	Pp3c17_16370	↑	Pectate lyase	0.98	6.45 × 10 ⁻⁸	
	Immune response	n.s.	Pp3c26_4220	↑	Alpha-dioxygenase	1.57	4.29 × 10 ⁻⁶	
		n.s.	Pp3c6_27380	↑	Spermidine synthase	1.00	4.89 × 10 ⁻⁶	
	Metal ion binding	Depleted	Pp3c7_6750	↓	Ferritin like receptor	-1.30	1.22 × 10 ⁻¹⁴	
	Photosynthesis	Depleted	Pp3c24_9670	↓	Early light-induced proteins	-2.07	1.48 × 10 ⁻²²	
Depleted		Pp3c11_7280	↓	Early light-induced proteins	-1.89	1.16 × 10 ⁻¹²		
<i>L. elongata</i> CU	Transcription factor	Enriched	Pp3c26_13260	↑	Ethylene response transcription factor	2.25	7.28 × 10 ⁻¹¹	
		Enriched	Pp3c6_2730	↑	HEX motif transcription factor	1.93	1.49 × 10 ⁻¹⁰	
		Enriched	Pp3c22_10160	↑	E2F/DP family helix DNA binding protein	2.95	2.18 × 10 ⁻¹⁰	
		Enriched	Pp3c9_470	↑	BIM1 motif transcription factor	1.82	6.92 × 10 ⁻¹⁰	
		Enriched	Pp3c11_6620	↑	RNA pol II transcription regulator	2.33	6.92 × 10 ⁻¹⁰	

(continued)

Table 1. (continued)

Coculture	Ontology	Regulation	Gene(s)	Expression	Annotation	Log ₂	P _{adj}
	Lipid transport	Enriched	Pp3c17_3860	↑	Cyclic DOF factor	2.57	6.92 × 10 ⁻¹⁰
		Enriched	Pp3c1_10000	↑	Hydroxymethylglutaryl-CoA reductase	1.40	9.05 × 10 ⁻¹¹
	Carbon metabolism	Enriched	Pp3c5_3730	↑	Allene oxide synthase	3.02	3.66 × 10 ⁻¹¹
		n.s.	Pp3c21_16620	↑	Xyloglucan glycosyltransferase	3.19	9.39 × 10 ⁻¹³
		n.s.	Pp3c20_13320	↑	Alpha-ketoglutarate sulfonate dioxygenase	1.60	3.28 × 10 ⁻¹¹
	Photosynthesis	n.s.	Pp3c7_5800	↓	GLK1 motif transcription factor	-2.69	1.25 × 10 ⁻¹³

For selected genes with particularly strong support and with implication in plant–fungal exchange but with ontologies not significantly represented (n.s.) were also included in this dataset.

activity has been reported as one of the first actions in the immune response to both abiotic and biotic stressors (Lu & Yao, 2018; Yang et al., 2022). Typically, during the early stages of infection photosynthetic activity is reduced and even after infection has passed transcript accumulation can remain low (Chen, Cui, et al., 2015; Hu et al., 2020; Scharte et al., 2005; Swarbrick et al., 2006; Yang et al., 2022).

We also investigated highly expressed individual genes outside the gene ontology (GO) categories, whose differential expression posed interesting considerations. Carbon metabolism genes stood out due to their distinct role in mediating plants–fungal symbiosis (Bonfante & Genre, 2010). Many of the highest supported and upregulated genes presented here are annotated with putative functionality in carbohydrate synthesis and cellulose/cell wall biosynthesis (Table 1). Additionally, there was also activation of three transcription factors which may be involved in the regulation of the previously highlighted gene ontologies. These included a WRKY, TIFY, and HEX transcription factor (Table 1). WRKY transcription factors are heavily represented and conserved among embryophytes, with nearly 40 copies in *P. patens*, and regulate the expression of abiotic stress, biotic stress, and developmental response (Bakshi & Oelmüller, 2014). In angiosperms, TIFY motif transcription factors have demonstrated the signaling of growth, development, and defense response, and we suspect similar activity here (Xia et al., 2017). *B. erionia* WT cocultures identified upregulation of a hydroxymethylglutaryl-CoA reductase (HMG-CoA; Table 1), encoding a key regulatory enzyme in the cytosolic mevalonate (MVA) terpenoid biosynthetic pathway (Table 1) (Friesen & Rodwell, 2004; Simkin et al., 2011). This gene is involved in the production of precursors of sterol biosynthesis, which are integral for membrane integrity and hormonal responses (Morikawa et al., 2009). The transcriptomic and histological responses described here parallel those recently described in the infection of *P. patens* with the broad spectrum

necrotrophic fungal pathogen *Botrytis cinerea* (Sclerotinia-ceae) and provide strong support for classifying *B. erionia* WT as pathogenic toward *P. patens* (Reboledo, 2021; Reboledo et al., 2020).

When cured of endobacteria, *B. erionia* CU loses the capacity for interaction with *P. patens*

In contrast to the response with *B. erionia* WT, the strain cured of the endobacterium reduced transcriptional response 40-fold when cocultured with *P. patens* (Figure 4). We detected 65 DEGs ($P_{adj} < 0.01$) in the presence of *B. erionia* CU, with only 46 upregulated genes and 19 downregulated genes (Data S2c). This limited set of genes still shows ontology enrichment in pathways for extracellular sensing and cell wall response (Data S4). There were no gene ontologies depreciated in *P. patens* when in coculture with *B. erionia* CU. We identified two upregulated transcription factors, which included an ethylene-responsive transcription factor and a MYB-like transcription receptor. Ethylene-responsive transcription factors are conserved throughout embryophytes and regulate many diverse regulatory pathways but predominantly are involved in response to external stimuli (Binder, 2020; Hall et al., 1977; Licausi et al., 2013; Nakano et al., 2015). Notably, the key committed step involved in *ent*-kaurene biosynthesis, encoded by the *ent*-kaurene synthase gene (Table 1), was also identified to be downregulated here.

Ent-kaurene has parallel functions to the gibberellins in angiosperms, which generally function in the regulation of developmental changes and response to pathogens and its downregulation here has implication for decreased environmental sensitivity (Hayashi et al., 2010; Miyazaki et al., 2011, 2018; Reboledo, 2021; Reboledo et al., 2020). Overall, *P. patens* response to *B. erionia* CU presents itself as relatively neutral, non-specific, and with no characteristics of plant–pathogen interaction. Therefore, *B. erionia* appears to require the endobacterium to retain pathogenicity.

L. elongata* WT cocultures demonstrate beneficial tendencies with *P. patens

When *L. elongata* WT was cocultured with *P. patens*, a total of 802 genes were differentially expressed ($P_{\text{adj}} < 0.01$), with 287 genes upregulated and 515 genes downregulated (Data S4). Of the upregulated genes, we identified enrichment in three ontologies: cytoskeletal reorganization, cell wall biogenesis and the synthesis of various polysaccharide pathways (Data S4). Complementing what was observed with microscopy, cytoskeletal rearrangement in *P. patens* may be occurring to harbor the *L. elongata* hyphae within plant cells but the cytoskeleton also plays dynamic roles in plant growth, development, and immune response (Wang et al., 2022). Additionally, we identified enrichment in cell wall biosynthesis (Data S4). Differentiation of cell wall activity likely has a related function to the differentiation of cytoskeletal rearrangement since both are implicated in cellular architecture. Upregulation for the synthesis of polysaccharides may be relevant in two different pathways due to the integral role of polysaccharides in the cell wall (Voiniciuc et al., 2018) or due to the essential role carbon exchange plays in plant–fungal mutualism (Bonfante & Genre, 2010). Alterations to carbon metabolism are generally indicative of plants–fungal symbiosis and the higher expression for these pathways here may suggest a positive interaction between these two species. Notable DEGs directly involved in carbon/photosynthesis included the Chlorophyll A/B binding protein, beta-1-3 glucanase, and GDP-fucose transferase (Table 1). These genes also suggest a heightened production of polysaccharides and also may indicate the upregulation of carbon metabolism. Further support for cross-kingdom interaction comes from DEGs encoding a formerly characterized alpha-dioxygenase (Table 1) (Groenewald & van der Westhuizen, 1997; Machado et al., 2015), which has been shown to participate in fungal infection response and plant development as well as a spermidine synthase (Table 1) which has implications in plant host defense against infection (Muel-ler, 1998; Stenzel et al., 2003; Takahashi & Kakehi, 2010).

Comparatively, *L. elongata* WT uniquely caused a disproportionately high number of downregulated genes including a depleted response to oxidative stresses, metal ion binding, and photosynthesis (Data S4). Reduced sensitivity to oxidative stresses is a common response induced by endophytic fungi in plant systems (Clay, 1988; Fontana et al., 2021; White & Torres, 2010). This relationship often embodies a mutualistic interaction by aiding both systems in defense, where fungi provide a heightened protection against abiotic stressors, specifically reactive oxygen species (ROS) (Clay, 1988; Fontana et al., 2021; White & Torres, 2010). This can be accompanied by fungal ROS mediation of the host, creating 'leaky' plant cells enabling easier access to nutrients by fungal endophytes, and could

further help explain the previously highlighted DEG, peccate lyase (Table 1) (Su, 2023; White & Torres, 2010). In plants, iron plays a key role in photosynthesis and the repression of its ontology here coincides with reduced photosynthetic activity (Data S4). Endophytic fungi have been reported to provide absorbable iron from the soil to their plant hosts (Verma et al., 2022). This may indicate that *P. patens* is receiving iron from *L. elongata* WT and consequently reducing iron binding, consistent with the observed repression of a ferritin-like receptor (Table 1). Like with *B. erionia* WT, we also detected a strong depletion of gene expression affiliated with photosynthesis in *P. patens* × *L. elongata* WT cocultures. This repression is likely again due to the important role of photosynthesis in general immune response. A distinction for *L. elongata* WT photosynthetic response compared to *B. erionia* WT is the affiliated deactivation of many early light-induced proteins (Table 1), which are usually activated in response to abiotic stress (Hutin et al., 2003). This complex suggests that an induced immune response is occurring, which, in combination with the lack of any asymptomatic phenotypes in photosynthetic tissue, may further point to the establishment of a beneficial interaction in *P. patens* × *L. elongata* WT cocultures.

Endobacterial absence in *L. elongata* CU influences its environmental colonization and shifts its subsequent interaction with *P. patens* to resemble *B. erionia* WT response

Physcomitrium patens in coculture with *L. elongata* CU had a total of 1053 DEGs ($P_{\text{adj}} < 0.01$), with 829 genes upregulated and 224 genes downregulated. While the quantity of DEGs was comparable to *L. elongata* WT, only 112 (10.3%) DEGs were shared between both *L. elongata* strains. In contrast, 583 (53.8%) DEGs were shared with *B. erionia* WT (Figure 4). We identified enrichment pathways in cell periphery/membrane activity, transcription factor activity, and lipid transport (Data S4). As with *B. erionia* CU, *L. elongata* CU also displayed no significant depletion of specific gene ontologies (Data S4). Due to the characteristic *L. elongata* CU sporulation phenotype and enrichment of cell periphery, the changes in *P. patens* gene expression may suggest mechanical or chemical interactions distinct from the other cocultures. As in *B. erionia* CU, the activation of the same ethylene response transcription factor (Table 1) could implicate signaling of pathogen response and/or alternative cell development in *P. patens* (Binder, 2020; Hall et al., 1977; Liccausi et al., 2013). The upregulation of phosphorelay signal transduction system and hybrid signal transduction histidine kinase (Table 1), involved in the regulation of osmotic and oxidative stress, may indicate that *L. elongata* CU is inducing a stress response cascade in *P. patens* (Carapia-Minero et al., 2017). Many of the

differentially expressed transcription factors identified here have homologs that are directly involved in other systems for growth, development, signaling, and differentiation. These included a HEX motif transcription factor (Soufi & Jayaraman, 2008), an E2F/DP family helix DNA binding protein (Müller et al., 2001; Mariconti et al., 2002), a BIM1 motif transcription factor specifically induced through membrane signaling (Yin et al., 2005), an RNA Pol II transcription regulator co-expressed with sporophyte development, and a cycling DOF factor (Ishida et al., 2014; Goralogia et al., 2017; Wei et al., 2018) (Table 1). We identified an allene oxide synthase (Table 1) with a suggested role in the jasmonate pathway and potential involvement in development and stress response (Stenzel et al., 2003). Also, we identified the same HMG-CoA reductase differentially expressed in *B. erionia* WT, indicating a connection to plant defense (Frien & Rodwell, 2004; Simkin et al., 2011).

Genes with lower transcript accumulation in *L. elongata* CU cocultures included a GLK1 motif transcription factor (Table 1) which has conserved function throughout embryophytes (and the algae *C. reinhardtii*), directly influencing chlorophyll biosynthesis (Gang et al., 2019; Waters et al., 2009; Yasumura et al., 2005). Represented as well were genes encoding for putative xyloglucan glycosyltransferase and an alpha-ketoglutarate sulfonate dioxygenase which are involved in carbon metabolism and more

specifically saccharide production. The upregulation of these genes could suggest that carbon exchange may be occurring or because the plant cell wall is a major sink for saccharides as well, these genes could also indicate major changes to cell wall structure.

Comparisons with the 'Gene Atlas Project' identify multiple novelties in *P. patens* expression

'The *Physcomitrella patens* gene atlas project: large-scale RNA-Seq based expression data' ('Gene Atlas Project') was published in response to the updated *P. patens* chromosome-scale genome assembly V3.3 in 2018 (Lang et al., 2018; Perroud et al., 2018). This resource was developed to identify specific trends involved in developmental stages, environmental conditions, and to support the reproducibility of RNA-sequencing in *P. patens* among different labs (Perroud et al., 2018). In contrast to the samples of the 'Gene Atlas Project', grown aseptically on defined growth media, we introduced two novel variables, fungal cocultures and growth on soil, a substrate closer resembling nature with no noticeable impact on *P. patens* or *Mortierella* growth. Comparisons between all samples (our 15 and the 99 'Gene Atlas Project' samples) were investigated using a PCA (Figure 5) (Supplementary Code S4). Our samples (Figure 5d) clustered tightly and distinctly from the original three major clusters 'gametophores'

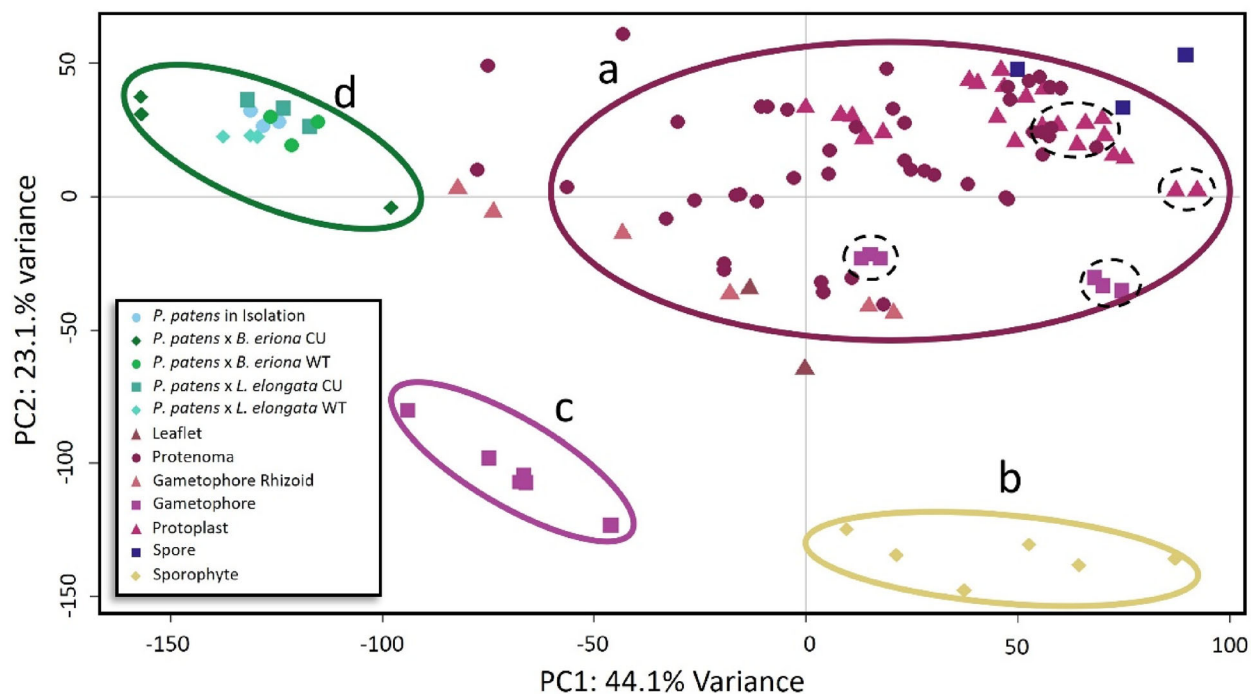


Figure 5. Principal component analysis (PCA) of transcripts per million mapped reads (TPM) of the 99 libraries from the 'Gene Atlas Project' (Perroud et al., 2018) and the 15 samples analyzed here.

Samples had four distinct clusters with various gametophore tissues [maroon, (a)], sexual tissues [yellow, (b)], high heat samples [purple, (c)], and samples grown on soil [green, (d)]. Circled with dotted ellipses are control groups from intra- and interlaboratory conditions with different media (Knop agar, Knop liquid, BCD agar). PC1 explains 44.1% of the variance and PC2 explains 23.1% of the variance.

(Figure 5a), ‘sporophytes’ (Figure 5b), and ‘strong stresses’ (Figure 5c). With PC1 explaining 44.1% of the variance, PC2 explaining 23.1% and PC3 explaining 11.1%, the inclusion of *P. patens* grown with fungi and on soil sufficiently shifted the original ‘Gene Atlas Project’ dispersion while maintaining the same clustering patterns from the originally explained variation (PC1: 78%, PC2: 10%, PC3: 6%) (Perroud et al., 2018). Growth on soil had a more defining signal than fungal cocultures, seen with the tight distribution of all 15 samples, including the control. Notably, the dotted circles in Figure 5 represent control experiments grown on the conventional liquid/solid BCD and Knop media with the same *P. patens* strain, genotype, and tissue types sampled as those grown here on soil (Cove et al., 2009; Perroud et al., 2018; Reski & Abel, 1985), which especially highlights the influence growth media has on gene expression. Explanatory variables for the expression difference of soil compared to lab-based agar/liquid media include supplements such as CaCO₃ and MgCO₃-rich dolomite, silicon, and organics through peat moss. Additionally, the soil provides moisture retention and structural aeration different than agar-based media. Although all samples tested here differed substantially from one another, growth on soil was the most influential factor in distinguishing their expression from the ‘Gene Atlas Project’ (Figure 5). The impact media has on *P. patens* expression is significant as ‘control’ samples grown on common *P. patens* growth media including BCD agar, BCDAT, Knop liquid/agar, Hoagland, and PpNH4 protoplast media all lead to distinct clustering of samples despite each recipe,

other than soil, having the similar composition (Data S7). Additionally, soil samples are on the same axis with PpNH4 and Hoagland-based media for PC1 (70.9% variance) and with Knop/BCD Agar samples for PC2 (19.6% variance) (Data S7). While using soil as a media here also leads to distinct clustering of samples from other media, they do not vary substantially to warrant their own category entirely. Comparatively, we see the difference in expression from growth on soil or growth on Knop agar is comparable to the difference from growth on BCD agar or Knop agar (Data S7). Differential expression analysis comparing our samples and the ‘Gene Atlas Project’ produced a total of 7450 significant DEGs ($P_{adj} < 0.0001$). Among these, 3873 were upregulated in our samples and 3577 were downregulated (Data S3a). Among upregulated genes, we identified enrichment in ubiquitin expression, transcription and translation, and nitrogen biosynthesis pathways (organonitrogen, peptides, and amides) (Data S4). From downregulated genes, we identified depleted activity in mitosis and cell division, endoplasmic reticulum activity, and Golgi apparatus activity (Data S4). A total of 2116 genes lacked any sign of expression specifically in our samples but were expressed in at least one other ‘Gene Atlas Project’ sample (Data S3e). Genes silenced in our system but expressed elsewhere saw enrichment in membrane processes and DNA transposition (Data S4). This included seven genes with expression conserved in all 99 ‘Gene Atlas Project’ samples and silenced in our system (Data S3e). Two of these genes function in endoplasmic reticulum transport (Pp3c9_10380, Pp3c12_8160) and three were

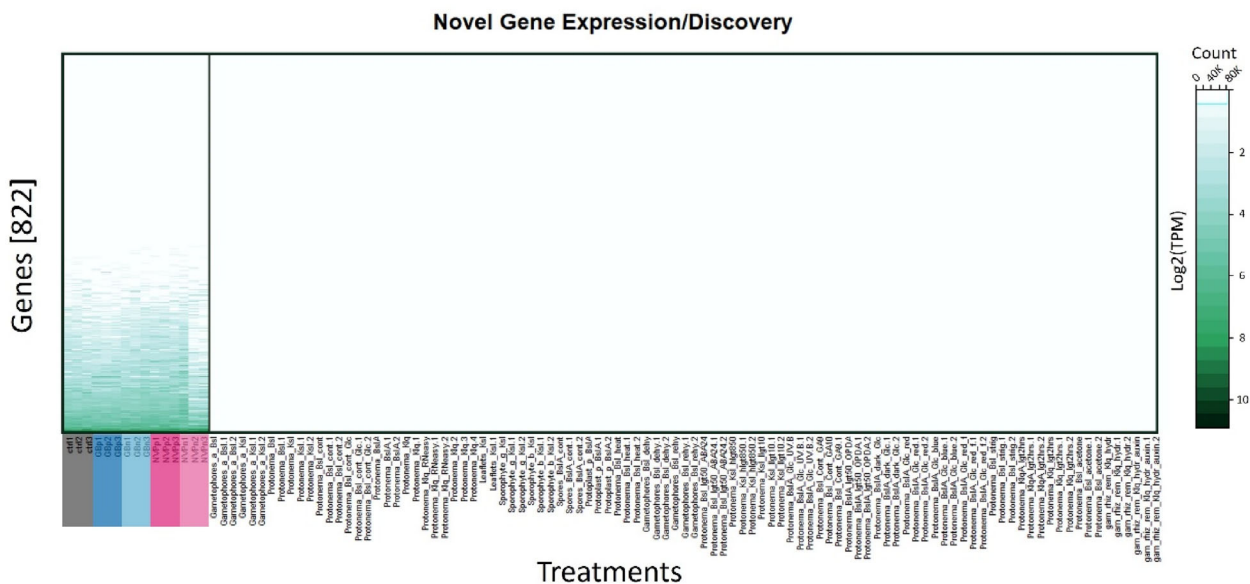


Figure 6. Heatmap of the 822 genes with mapped reads to the dataset were presented here and absent among all ‘Gene Atlas Project’ samples. Rows ordered based on the total sum of gene expression per gene. Columns represent the 114 sample conditions. Control groups (black), *Benniella. erionia* WT (dark blue), *B. erionia* CU (light blue), *Linnemannia elongata* WT (magenta), *L. elongata* CU (pink), and ‘gene atlas samples’ (white). Expression in TPM is measured based on a log₂ scale where the darker shade of green indicates more expression and white indicates no expression.

involved in the regulation of the central dogma (Pp3c1_24700, Pp3c11_25450, Pp3c10_6100). In contrast, novel expression exclusive to the current study yielded a total of 822 genes (Figure 6). Among those, 55 genes (6.7%) were not scaffolded to a chromosome, representing over a threefold higher abundance than what would be expected based on the transcriptomic makeup. Of those 822 genes, 26% had a significantly high differential expression with the most highly supported gene (Pp3c15_19571) having an average of 781 TPM (in the top 1% of genes expressed). Among genes with novel expression, we detected enrichment in pathways involved in RNA polymerase II activity, cell shape regulation, and beta (1,3)-D-glucan biosynthesis activity (Data S4). While RNA polymerase II activity is most well-known for its role in the production of messenger RNA, it also plays a dynamic and conserved role in plant pathogen response and its representation here likely shares both functionalities here (Li et al., 2014). A sub-class of RNA-polymerase II, the RNA-directed RNA polymerases, also have utility in forming small interfering RNA (siRNA) (Du et al., 2022; Hunter et al., 2013) and a putative RNA-directed RNA polymerase was included among our identified genes (Pp3c6_8521). Generally, siRNAs function against the invasion of foreign entities, alternative gene regulation, and control of transpositional elements (Castel & Martienssen, 2013; Du et al., 2022), which may parallel the unique challenges presented in our conditions. Also, DNA-transposition was one of the few ontologies underrepresented in our system and its reduced transposition may be due to the presence of siRNA. Enrichment of cell shape morphology detected in all samples may imply the necessity for certain cellular features for soil-specific conditions. Genes putatively involved in beta (1,3)-D-glucan biosynthesis have a presumed involvement in cell wall structure (Douglas, 2001; Roberts et al., 2012, 2018) and plant defense (Vega-Sánchez et al., 2013).

CONCLUSION

Here we report that the Mortierellaceae species *B. erionia* and *L. elongata* are both capable of endophytic interactions with *P. patens*, albeit subtle and possibly dependent on endobacteria. The ability of these fungi to interact with *P. patens* is largely dependent on endobacterial presence and absence, which changes both the plant's phenotypic and transcriptomic response. Current understandings of how endobacteria influence their fungal host and the subsequent effects that these have on their environment are still limited, and because of this, their influence on *P. patens* interaction is notable, particularly with MRE in *B. erionia*. Interactions between any two organisms are environmentally dependent and may be beneficial or adversarial depending on those conditions (Bonfante & Genre, 2010; Dickie et al., 2013; Du et al., 2019; Eastburn et al., 2011; Giaque & Hawkes, 2013) and as such we are just

beginning to uncover the complexities of potential relationships with *P. patens* and fungi in Mortierellaceae.

Comparison with the 'Gene Atlas Project' indicated distinct changes to gene expression caused by different growth conditions (soil vs. common lab-based media). Comparisons across our work and that of the 'Gene Atlas Project' yielded the discovery of 822 genes with novel expression, and 7 genes which previously were otherwise constitutively on, and an updated 'Gene Atlas' reference with the appending of our data providing more context in future work along with methodology for further expansion (Data S3a,b; Supplementary Code S4). While the mechanisms of how plants initially colonized land remains a mystery, the biodiversity and response captured by the second largest clade of land plants, the bryophytes, helps to provide further gravity to the influential role fungi played in making that possible. In conclusion, the exchange between plant hosts and fungal symbionts, and the evolution of those exchanges, are dynamic, competitive, and conditional.

MATERIALS AND METHODS

Bright field microscopy of *P. patens* and *Mortierella* in coculture

Physcomitrium patens (Gransden 2004; strain Pp40001) and *L. elongata* wildtype (WT), *L. elongata* cured of BRE (CU), *B. erionia* wildtype (WT) and *B. erionia* cured of MRE (CU) were cocultured on opposite halves of BCD agar media (1 mM MgSO₄, 1.84 mM KH₂PO₄, 10 mM KNO₃, 12.5 mg FeSO₄·7H₂O, 7 g Agar, 1 ml Hoagland's A-Z trace element solution, H₂O to 1L) for 2 weeks (Ashton & Cove, 1977; Wang & He, 2015). *B. erionia* and *L. elongata* were cured of endobacteria in previous work by cycling between liquid and agar media for 1-week intervals over 15 weeks with a combination of four antibiotics (80 µg ml⁻¹ ampicillin, 50 µg ml⁻¹ kanamycin, 50 µg ml⁻¹ streptomycin, and 120 µg ml⁻¹ ciprofloxacin) (Desirò et al., 2018; Uehling et al., 2017). The resulting fungal strains were then confirmed for the absence of endobacteria through sequence verification. Whole plant-fungal cocultures, which mainly consisted of *P. patens* protonema, and to a lesser extent *P. patens* rhizoid and leaflets (all asexual tissues) along with fungal hyphae, were collected by scraping all tissue off the surface of the plate with tweezers, placing in 1.5 ml Eppendorf tubes, and cleared with 1 ml formalin-aceto-alcohol (FAA) solution (50 ethanol:5 glacial acetic acid:10 formalin:35 H₂O). The cocultures were then placed under a vacuum for 30 min and stored in the dark overnight. The next day, the FAA solution was removed with a pipette, then the tissue was stained with 1 ml 1% Chlorazol Black E for 24 h. Samples were destained with 25, 50, and 75, ethanol solutions each for 20 min, then stored in 100% ethanol solution until microscopy. Samples were then placed on a microscope slide with glycerol and viewed with a bright field microscope (Model: Leica DM750) (Figure 2; Data S6).

Automated phenotyping of *P. patens* and *Mortierella* using RaspberryPi

Physcomitrium patens (Gransden 2004; strain Pp40001) was inoculated on 100 g wet Redi-earth soil in 1-L, wide-mouth mason jars,

under fluorescent lights, on top of a black tarp, with white walls surrounding the experiment. A sterilized, white, metal thumbtack was placed in the center of the soil for each sample to correct for white balance. Samples were watered every 14 days (or as needed to keep soil damp), with 10 mL distilled water. One-piece, twist-top, wide mouth lids were used and had two, 1 cm diameter holes drilled, for camera placement and watering, respectively. *P. patens* in BCD-agar were blended until homogenous at the day of inoculation, and evenly dispersed among samples. The four fungal strains were grown independently for inoculation on 2 g of perlite with 10 ml of minimal malt extract (5 g L⁻¹ malt extract, 0.25 g L⁻¹ yeast extract) liquid media for 2 weeks. Fungal treatments were randomly selected for inoculation to jars following the 2-week growth phase. In each jar, 2 g of saturated, colonized perlite was dispersed to their respective treatment (10 control, 8 *P. patens* × *B. erionia* WT, 8 *P. patens* × *L. elongata* WT, 7 *P. patens* × *B. erionia* CU, 7 *P. patens* × *L. elongata* CU). The control treatment was inoculated with 2 g of perlite and sterile malt extract media.

Monitoring of growth occurred with RaspberryPi Microcomputers 3 ModelB V1.2, which were initialized following online instructions,¹ and all devices were fitted with an Arducam Multi Camera Adapter Module V2.1 with four Raspberry Pi V2.1 Cameras. Scripts to run the multi-camera adapter and camera were downloaded and set up following instructions for this specific RaspberryPi hardware.² Images were automatically captured daily at 12:00 p.m. EST (Data S1a). Double-sided 2 × 2 cm scotch foam tape with an 8 mm diameter cut hole was placed on jar lids to secure cameras with a perpendicular view ~15 cm away from each sample then secured to position with tape.

Image analysis using PlantCV

Images were annotated to include key information, i.e., their origin and time of image capture Cam#_lens.#_YEAR-MM-DD_HH-MM.jpg (ex: Cam1_lens_1_2021-08-13_12-00.jpg). Python script (Supplementary Code S1) for quantifying green pixels in each image ran in Jupyter Notebook (Kluyver et al., 2016). PlantCV installation³ was done following Anaconda⁴-specific instructions (Berry et al., 2018; Gehan et al., 2017). Necessary dependencies were imported for analysis (os [v3.7.6], numpy [v1.18.1], cv2 [v3.4.9], matplotlib [v3.1.3], plantcv [v3.8.0], pandas [v1.0.1], glob [v3.7.6]). Each picture was then loaded and labeled based on treatment, date, computer, and camera. The white thumbtack centered in each mason jar was used to correct for white balance. Each image was converted from RGB (red, green, blue) to the LAB (lightness, magenta/green, blue/yellow) color space. The threshold for plant health was designated as anything in the pixel value range among the 'A' (green-magenta) values between 121 and 255. This range was selected due to it distinguishing only healthy, green moss tissue. Clusters of pixel groups less than 100 were removed and dilated to reduce noise. Final appended counts along with treatment, date, computer, and camera were then exported as a .csv for data visualization and evaluation (Data S1b).

Propagation of *P. patens* in coculture with Mortierellaceae species for RNA extraction

Samples were grown on autoclaved Redi-earth mix, inoculated with liquid BCD media in sterile glass jars with 0.5- μ m pore vents under 50 μ mol LED lights over the course of 35 days with fungal inoculation occurring on day 10. The 25 days spent in coculture provided time for fungi and plants to sufficiently overcome transplant stresses and naturally colonize the soil together (to avoid differential expression and variation that may be caused solely by

changing environments). The five experimental conditions were grown in triplicate with *P. patens* (Genotype: Grandsen 2004; strain: Pp40001) grown in seclusion, cocultured with *L. elongata* strains containing or cured of endobacteria (WT/CU), and cocultured with *B. erionia* strains containing or cured of endobacteria (WT/CU). Fungi in isolation were also cultivated, however, tissue retrieved was insufficient for RNA sequencing. Using tweezers, samples were extracted and separated from the soil 25 days after inoculation, removing growth substrate while maintaining *P. patens* rhizoid and fungal hyphae structures. Samples were flash frozen in liquid N₂ in 2 ml Eppendorf tubes and stored at –80°C until RNA extraction.

RNA extraction and quality control for Illumina library preparation

A phenol–chloroform-based RNA extraction was performed as described in previous work (Kolossova et al., 2004) but adapted to 100 mg of plant tissue. After extraction, 1 μ l RNA was run on a 1% agarose gel to confirm integrity. Samples were treated with DNase following the manufacturer's instructions (Thermo Fisher Scientific, Waltham, MA, USA; Product AM1907). Submitted RNA was quality checked with an Agilent 2100 (Agilent Technologies, Santa Clara, CA, USA) Flowcell Bioanalyzer (RNA integrity value 8.11 ± 0.15 [95% CI]), DeNovix DS-11 (DeNovix, Wilmington, DE, USA) Nanodrop (273.8 ± 41.3 ng μ l⁻¹ [95% CI]), and Qubit 2.0 Fluorometer.

RNA sequencing, processing, alignment, and data management

Plate-based RNA sample prep was performed on the PerkinElmer (Shelton, CT, USA) Sciclone NGS robotic liquid handling system using Illumina's TruSeq Stranded mRNA HT sample prep kit (Illumina, San Diego, CA, USA) utilizing poly-A selection of mRNA following the protocol outlined by Illumina in their user guide: https://support.illumina.com/sequencing/sequencing_kits/truseq-stranded-mrna.html, and with the following conditions: total RNA starting material was 1 μ g per sample and eight cycles of PCR was used for library amplification. The prepared libraries were then quantified using the KAPA Illumina library quantification kit (Roche, Basel, Switzerland) and run on a LightCycler 480 real-time PCR instrument (Roche). The quantified libraries were then multiplexed and the pool of libraries was then prepared for sequencing on the Illumina NovaSeq 6000 sequencing platform using NovaSeq XP v1 reagent kits (Illumina), S4 flow cell, following a 2 × 150 indexed run recipe (Modi et al., 2021). We generated a total of 664 million paired reads (per sample: $49M \pm 3.9M$ [95% CI]) and data is available on the JGI online genome database (gold.jgi.doe.gov/projects; GOLD Project ID Gp0332982-Gp0332996) and the NCBI SRA database (PRJNA807682). All reads were mapped back to *P. patens* genome version 3.3 CDS file 2018 (Ppatens_318_V3.3.cds-fa.gz; Phytozome; NCBI Taxonomy ID: 3218) (*P. patens* transcriptome) (Lang et al., 2018), Filtered Mortierella GBAus27b CDS file (MorGBAus27b_1_GeneCatalog_CDS_20170422.fa.gz, MycoCosm; NCBI Taxonomy ID: 1954212) (*B. erionia* transcriptome) (Chang et al., 2022), and filtered *Mortierella* NVP64 CDS file (MoeNVP64_1_GeneCatalog_CDS_20190403.fa.gz; MycoCosm; NCBI Taxonomy ID: 2684331) (*L. elongata* transcriptome). Prior to mapping, meta-transcriptomes were created representing their respective environmental conditions by concatenating all genes from *P. patens* with either the *B. erionia* transcriptome or *L. elongata* transcriptome when applicable. Supplementary bash script (Supplementary Code S2a,b) was submitted to the Michigan State University High Performance Computing Center (MSU HPC). The transcriptome and meta-transcriptomes (*P. patens*; *P. patens* × *B.*

erionia; *P. patens* × *L. elongata*) were indexed using Salmon (v1.2.1) and the 'salmon index' function to create reference libraries for downstream read quantification. Raw reads were split into forward and reverse read files, raw QC reports were generated with FastQC (v0.11.7), low-quality reads and adapters were removed using FastP (v0.21.0) which maintained $97.33 \pm 0.64\%$ (95% CI) of the original sequence (Andrews, 2010; Chen et al., 2018; Patro et al., 2017). Trimmed QC reports were again generated with FastQC, and filtered reads were mapped to their respective index using the 'salmon quant' function (Andrews, 2010). In total there were five treatments, each in triplicate (JGI Sample Barcode; *P. patens*: CUTON, CUTOO, CUTOP; *P. patens* × *B. erionia* WT: CUTOS, CUTOT, CUTOU; *P. patens* × *B. erionia* CU: CUTOV, CUTOX, CWYAU; *P. patens* × *L. elongata* WT: CUTOZ, CUTPA, CUTPB; *P. patens* × *L. elongata* CU: CUTPC, CUTPG, CUTPH) (Data S2a).

Differential gene expression analysis using DESeq2

Expression of *P. patens* genes from each treatment were differentiated and determined as significant using DESeq2 (v1.26.0) (Supplementary Code S3) (Love et al., 2014). The *P. patens* mapped read dataset (Data S2a) was used as an input after formatting with tximport (v1.22.0), to correct for multiple isoforms across samples (Soneson et al., 2016). The algorithm modeled relative library depth, dispersion of individual gene counts, and significance of coefficients, all of which were used to determine library size and dispersion corrected negative binomial general linearized model. Genes were considered significant if they demonstrated high differential expression differences based on Bonferroni ($P_{adj} < 0.01$) (Data S2b–e).

Comparative analysis between the *P. patens* 'Gene Atlas Project'

The quantified reads per kilobase per million (RPKM) datasets from 'The *Physcomitrella patens* Gene Atlas Project' were downloaded to compare our 15 samples to their 99 *P. patens* samples representing various tissues, treatments, growth stages, and laboratory biases to untangle globally shared trends in expression (Perroud et al., 2018). RPKM values were converted to transcript per million (TPM) using the following equation on the dataset: $TPM = \frac{RPKM}{\sum RPKM} \times 10^6$ (Data S3a,b; Supplementary Code S4) because TPM is a unitless metric and resembles a percentage based system, it corrects for varying library sizes, and serves as a better tool for inter-sample comparison (Zhao et al., 2020). The dataset was simplified by removing genes with summed expression less than 20 TPM across all samples ($\sum_{15} TPM < 20$), which reduced the data-

set by 51.47% (16256/31581). Differential expression of samples between results reported here and within the 'Gene Atlas Project' were compared using DESeq2 (Data S3c; Supplementary Code S4) (Love et al., 2014). A PCA was performed to identify clustering based on expression to identify similarities or differences between our samples and the 'Gene Atlas Project'. Additionally, comparisons were made across all samples with a $\sum_{99} TPM = 0$ among all

'Gene Atlas Project' samples and then compared to our samples where $\sum_{15} TPM \neq 0$ to identify any novel gene expression (Data S3d).

This comparison was also made in reverse to identify which genes were silenced in our samples, in which $\sum_{15} TPM = 0$ and $\sum_{99} TPM \neq 0$ among the 'Gene Atlas Project' (Data S3e).

Comparisons based on common *P. patens* media sampled 41 libraries from gametophore tissues grown on BCD Agar (five), BCDAT (six), Hoagland (six), Knop agar (eight), Knop liquid (eight), PpNH4 protoplast solution (five), and soil (three). This was taken

from five different projects (PRJNA751102, PRJNA880579, PRJNA723997, PRJNA259147, and PRJNA807682) (Data S7) (Causier et al., 2023; Garcias-Morales et al., 2023; Otero-Blanca et al., 2021; Perroud et al., 2018). Select SRA 'control' reads from each project were downloaded using SRA-toolkit (v3.0.3), trimmed with Fastp (v0.21.0), the *P. patens* transcriptome was again indexed and used for mapping reads with Salmon (v1.8.0), and finally quantified read files were merged using the salmon merge function (Supplementary Code S5). PCA was generated as before using Supplementary Code S4, but with the media-based quant file as an input and classification of each variable based on media (Data S7; Supplementary Code S5).

M. elongata NVP64 genome and transcriptome sequencing, assembly and annotation

The *M. elongata* NVP64 genome was sequenced using the PacBio (Pacific Biosciences, Menlo Park, CA, USA) Sequel platform. In this study, 5 µg of genomic DNA was sheared to >10 kb using Covaris (Woburn, MA, USA) g-Tubes. The sheared DNA was treated with exonuclease to remove single-stranded ends and DNA damage repair mix followed by end repair and ligation of blunt adapters using SMRTbell Template Prep Kit 1.0 (Pacific Biosciences). The library was purified with AMPure PB beads. PacBio Sequencing primer was then annealed to the SMRTbell template library and sequencing polymerase was bound to them using Sequel Binding kit 3.0. The prepared SMRTbell template libraries were then sequenced on a Pacific Biosciences's Sequel sequencer using v3 sequencing primer, 1M v3 SMRT cells, and Version 3.0 sequencing chemistry with a 1 × 360 sequencing movie run time. Filtered subread data was assembled with Falcon version (pb-assembly 0.0.2, falcon-kit 1.2.3, pyflow 2.1.0) (<https://github.com/PacificBiosciences/FALCON>) to generate an initial assembly. Mitochondrial sequence was assembled separately from the Falcon pre-assembled reads (preads) using an in-house tool (assemble-mito.sh), used to filter the preads, and polished with Arrow version SMRTLink (v6.0.0.47841) (<https://github.com/PacificBiosciences/GenomicConsensus>). A secondary Falcon assembly was generated using the mitochondria-filtered preads, improved with finisherSC (v2.1; Lam et al., 2015), and polished with Arrow version SMRTLink (v6.0.0.47841) (<https://github.com/PacificBiosciences/GenomicConsensus>). Completeness of the euchromatic portion of the genome assembly was assessed by aligning assembled consensus RNA sequence data with bbtools (v38.41) bbmap.sh ($k=13$ maxindel = 100 000 customtag ordered nodisk) and bbest.sh (fraction = 85) (<http://sourceforge.net/projects/bbmap>). Contigs less than 1000 bp were excluded.

We additionally sequenced and assembled a de-novo transcriptome for *M. elongata* NVP64, which provided RNA evidence for improved gene calling. Plate-based RNA sample prep was performed on the PerkinElmer Sciclone NGS robotic liquid handling system using Illumina's TruSeq Stranded mRNA HT sample prep kit utilizing poly-A selection of mRNA following the protocol outlined by Illumina in their user guide (http://support.illumina.com/sequencing/sequencing_kits/truseq_stranded_mrna_ht_sample_prep_kit.html) and with the following conditions: total RNA starting material was 1 µg per sample and eight cycles of PCR was used for library amplification. The prepared library was quantified using KAPA Biosystem's next-generation sequencing library qPCR kit (Roche) and run on a Roche LightCycler 480 real-time PCR instrument. The quantified library was then multiplexed with other libraries, and the pool of libraries was then prepared for sequencing on the Illumina HiSeq sequencing platform utilizing a TruSeq paired-end cluster kit, v4, and Illumina's cBot

instrument to generate a clustered flow cell for sequencing. Sequencing of the flow cell was performed on the Illumina HiSeq 2500 sequencer using HiSeq TruSeq SBS sequencing kits, v4, following a 2 × 150 indexed run recipe. Raw fastq file reads were filtered and trimmed using the JGI QC pipeline resulting in the filtered fastq file. Using BBDuk,⁵ raw reads were evaluated for artifact sequence by kmer matching (kmer = 25), allowing 1 mismatch and detected artifact was trimmed from the 3' end of the reads. RNA spike-in reads, PhiX reads, and reads containing any Ns were removed. Quality trimming was performed using the phred trimming method set at Q6. Finally, following trimming, reads under the length threshold were removed (minimum length 25 bases or 1/3 of the original read length – whichever is longer). Filtered fastq files were used as input for de novo assembly of RNA contigs. Reads were assembled into consensus sequences using Trinity (v2.3.2) (Grabherr et al., 2011). Trinity was run with the --normalize_reads (In-silico normalization routine) and --jaccard_clip (Minimizing fusion transcripts derived from gene dense genomes) options. Incorporating this de-novo transcriptome and filtered RNAseq reads, the *M. elongata* NVP 64 genome was then annotated using the JGI annotation pipeline (Grigoriev et al., 2014).

GO enrichment analysis

Gene ontology enrichment was categorized using g:Profiler by submitting the separated list of significant up- or down-regulated genes generated with DESeq (Data S2b–e) for each experimental condition (Data S4). The g:Profiler software was used to identify significantly differentiated GO terms for the four fungal treatments and *P. patens* and overrepresented terms between our samples and the 'Gene Atlas Project' (Raudvere et al., 2019; Reimand et al., 2007).

ACKNOWLEDGEMENTS

We would like to thank Alan Yocca and Patrick Edger for their recommendations and mentoring in phylogenetics; Aparajita Banerjee, Malik Sankofa, and Balindile Motsa for their assistance in maintaining and growing *P. patens* strains; Sean Johnson, Reid Longley, and Natalie VandePol for their help and recommendations for genetic analysis. The work (proposal: 10.46936/10.25585/60001086) conducted by the U.S. Department of Energy Joint Genome Institute (<https://ror.org/04xm1d337>), a DOE Office of Science User Facility, is supported by the Office of Science of the U.S. Department of Energy operated under Contract No. DE-AC02-05CH11231. DM, GB, and BH acknowledge support for this project from the NSF Dimensions of Biodiversity Grant (DEB 1737898) and the NSF-funded doctoral student training grant Integrated Training Model in Plant and Compu-Tational Sciences (IMPACTS). BH and GB acknowledge funding from the Great Lakes Bioenergy Research Center, U.S. Department of Energy, Office of Science, Office of Biological and Environmental Research under Award Number DE-SC0018409 and support from the Department of Biochemistry and Molecular Biology startup funding and support from AgBioResearch (BH = MICL02454; GB = MICL02416). GB also acknowledges support from the US Department of Energy (DOE) Biological and Environmental Research (BER) and Biological System Science Division (BSSD) under the grant number LANLF59T. BH gratefully acknowledges support from the MSU James K. Billman, Jr. MD endowment. We collectively acknowledge that Michigan State University occupies the ancestral, traditional, and contemporary Lands of the Anishinaabeg – Three Fires Confederacy of Ojibwe, Odawa, and Potawatomi peoples. In particular, the University resides on Land ceded in the 1819 Treaty of Saginaw. We recognize, support, and advocate for the sovereignty of Michigan's 12 federally recognized Indian nations, for historic Indigenous communities in Michigan,

for Indigenous individuals and communities who live here now, and for those who were forcibly removed from their Homelands. By offering this Land Acknowledgement, we affirm Indigenous sovereignty and will work to hold Michigan State University more accountable to the needs of American Indians and Indigenous peoples.

CONFLICT OF INTEREST

The authors declare no conflict of interest.

SUPPORTING INFORMATION

Additional Supporting Information may be found in the online version of this article.

- Data S1.** Supp.1a.Physco_photos.tar.gz.
- Data S1b.** Supp.1b.Photo_Pixel_Quantification.csv.
- Data S2a.** Supp.2a.Physco_quants.tar.gz.
- Data S2b.** Supp.2b.Ppatens_Berionawt_DESeq.csv.
- Data S2c.** Supp.2c.Ppatens_Berionacu_DESeq.csv.
- Data S2d.** Supp.2d.Ppatens_Lelongatawt_DESeq.csv.
- Data S2e.** Supp.2e.Ppatens_Lelongatacu_DESeq.csv.
- Data S3a.** Supp.3a.Perroud_Mathieu.tar.gz.
- Data S3b.** Supp.3b.Perroud_Mathieu.csv.
- Data S3c.** Supp.3c.Significant_Perroud.csv.
- Data S3d.** Supp.3d.Novel_Expression_Perroud_v_Mathieu.csv.
- Data S3e.** Supp.3e.Novel_Silencing_Perroud_v_Mathieu.csv.
- Data S4.** Supp.4.Gene_Ontology_Reports.xlsx.
- Data S5a.** Supp.5a.Algae_quants.tar.gz.
- Data S5b.** Supp.5b.Arabidopsis_quants.tar.gz.
- Data S5c.** Supp.5c.Orthogroup_Significant_hits_overlap.xlsx.
- Data S5d.** Supp.5d.Orthogroups.tsv.
- Data S5e.** Supp.5e.SingleCopy_Orthogroups_all.tsv.
- Data S5f.** Supp.5f.SingleCopy_Orthogroups_AT_PP.tsv.
- Data S5g.** Supp.5g.SingleCopy_Orthogroups_CR_PP.tsv.
- Data S6.** Supp.6.Additional_Microscopy_Photos.tar.gz.
- Data S7.** Supp.7.Media_Effects_On_Ppatens_PCA.pdf.
- Data S8.** Supp.8.SYM_gene_hits.txt.
- Data S9.** Supp.9.Mortierella_elongata_NVP64_genome_stats.xlsx.
- Supplementary Code S1.** Supp.1.Green_Pixel_Quantification.ipynb.
- Supplementary Code S2a.** Supp.2a.Salmon_analysis.sh.
- Supplementary Code S2b.** Supp.2b.Split_files.pl.
- Supplementary Code S3.** Supp.3.DESeq2_physco_v_Mort.R.
- Supplementary Code S4.** Supp.4.Perroud_Mathieu_comparisons.r.
- Supplementary Code S5.** Supp.5.Media_based_analysis.tar.gz.

OPEN RESEARCH BADGES



This article has earned Open Data and Open Materials badges. Data and materials are available at <https://datadryad.org/stash/share/2g3gZefPksJaPGILpc8d7gMWqmniLAnQkCI9QRo79c> and <https://zenodo.org/record/8067745>.

DATA AVAILABILITY STATEMENT

The following Supplementary Data have been deposited at <https://datadryad.org/stash/share/2g3gZefPksJaPGILpc8d7g>

MWqmniILAnQkCl9QRo79c. The following Supplementary Code has been deposited at <https://zenodo.org/record/8067745>. The genome of *Linnemania elongata* was submitted to NCBI GenBank and will be accessible as soon as the data is processed.

Endnotes

¹ <https://projects.raspberrypi.org/en/projects/raspberry-pi-setting-up>.

² https://www.arducam.com/downloads/RaspCAM/RaspberryPi_Multi_Camera_Adapter_Module_UG.pdf.

³ <https://plantcv.readthedocs.io/en/latest/installation/>.

⁴ <https://www.anaconda.com/>.

⁵ <https://sourceforge.net/projects/bbmap/>.

REFERENCES

- Akiyama, K., Matsuzaki, K. & Hayashi, H. (2005) Plant sesquiterpenes induce hyphal branching in arbuscular mycorrhizal fungi. *Nature*, **435**(7043), 824–827. Available from: <https://doi.org/10.1038/nature03608>
- Alabid, I., Glaeser, S.P. & Kogel, K.-H. (2019) Endofungal bacteria increase fitness of their host fungi and impact their association with crop plants. *Current Issues in Molecular Biology*, **30**, 59–74. Available from: <https://doi.org/10.21775/cimb.030.059>
- Allan, C., Morris, R.J. & Meisrimler, C.-N. (2022) Encoding, transmission, decoding, and specificity of calcium signals in plants. *Journal of Experimental Botany*, **73**(11), 3372–3385. Available from: <https://doi.org/10.1093/jxb/erac105>
- Andrews, S. (2010) *FastQC: a quality control tool for high throughput sequence data*. Available from: <https://www.bioinformatics.babraham.ac.uk/projects/fastqc/> [Accessed March 2023].
- Ashton, N.W. & Cove, D.J. (1977) The isolation and preliminary characterization of auxotrophic and analogue resistant mutants of the moss, *Physcomitrella patens*. *Molecular and General Genetics MGG*, **154**(1), 87–95. Available from: <https://doi.org/10.1007/BF00265581>
- Bakshi, M. & Oelmüller, R. (2014) WRKY transcription factors. *Plant Signaling & Behavior*, **9**, e27700. Available from: <https://doi.org/10.4161/psb.27700>
- Becker, L.E. & Cubeta, M.A. (2020) Increased flower production of *Calibrachoa x hybrida* by the soil fungus *Mortierella elongata*. *Journal of Environmental Horticulture*, **38**(4), 114–119. Available from: <https://doi.org/10.24266/0738-2898-38.4.114>
- Berry, J.C., Fahlgren, N., Pokorny, A.A., Bart, R.S. & Velez, K.M. (2018) An automated, high-throughput method for standardizing image color profiles to improve image-based plant phenotyping. *PeerJ*, **6**, e5727. Available from: <https://doi.org/10.7717/peerj.5727>
- Besserer, A., Puech-Pagès, V., Kiefer, P., Gomez-Roldan, V., Jauneau, A., Roy, S. *et al.* (2006) Strigolactones stimulate arbuscular mycorrhizal fungi by activating mitochondria. *PLoS Biology*, **4**(7), e226. Available from: <https://doi.org/10.1371/journal.pbio.0040226>
- Binder, B.M. (2020) Ethylene signaling in plants. *The Journal of Biological Chemistry*, **295**(22), 7710–7725. Available from: <https://doi.org/10.1074/jbc.REV120.010854>
- Bonfante, P. & Genre, A. (2010) Mechanisms underlying beneficial plant–fungus interactions in mycorrhizal symbiosis. *Nature Communications*, **1**(1), 48. Available from: <https://doi.org/10.1038/ncomms1046>
- Bressendorff, S., Azevedo, R., Kenchappa, C.S., Ponce de León, I., Olsen, J.V., Rasmussen, M.W. *et al.* (2016) An innate immunity pathway in the moss *Physcomitrella patens*. *The Plant Cell*, **28**(6), 1328–1342. Available from: <https://doi.org/10.1105/tpc.15.00774>
- Carapia-Minero, N., Castelán-Vega, J.A., Pérez, N.O. & Rodríguez-Tovar, A.V. (2017) The phosphorelay signal transduction system in *Candida glabrata*: an in-silico analysis. *Journal of Molecular Modeling*, **24**(1), 13. Available from: <https://doi.org/10.1007/s00894-017-3545-z>
- Castel, S.E. & Martienssen, R.A. (2013) RNA interference in the nucleus: roles for small RNAs in transcription, epigenetics and beyond. *Nature Reviews Genetics*, **14**(2), 100–112. Available from: <https://doi.org/10.1038/nrg3355>
- Causier, B., McKay, M., Hopes, T., Lloyd, J., Wang, D., Harrison, C.J. *et al.* (2023) The TOPLESS corepressor regulates developmental switches in the bryophyte *Physcomitrium patens* that were critical for plant terrestrialisation. *The Plant Journal*, **115**(5), 1331–1344. Available from: <https://doi.org/10.1111/tpj.16322>
- Chang, Y., Wang, Y., Mondo, S., Ahrendt, S., Andreopoulos, W., Barry, K. *et al.* (2022) Evolution of zygomycete secretomes and the origins of terrestrial fungal ecologies. *iScience*, **25**(8), 104840. Available from: <https://doi.org/10.1016/j.isci.2022.104840>
- Chen, J., Gutjahr, C., Bleckmann, A. & Dresselhaus, T. (2015) Calcium signaling during reproduction and biotrophic fungal interactions in plants. *Molecular Plant*, **8**(4), 595–611. Available from: <https://doi.org/10.1016/j.molp.2015.01.023>
- Chen, S., Zhou, Y., Chen, Y. & Gu, J. (2018) fastp: an ultra-fast all-in-one FASTQ preprocessor. *Bioinformatics*, **34**(17), i884–i890. Available from: <https://doi.org/10.1093/bioinformatics/bty560>
- Chen, Y.-E., Cui, J.-M., Su, Y.-Q., Yuan, S., Yuan, M. & Zhang, H.-Y. (2015) Influence of stripe rust infection on the photosynthetic characteristics and antioxidant system of susceptible and resistant wheat cultivars at the adult plant stage. *Frontiers in Plant Science*, **6**, 779. Available from: <https://doi.org/10.3389/fpls.2015.00779>
- Clay, K. (1988) Fungal endophytes of grasses: a defensive mutualism between plants and fungi. *Ecology*, **69**(1), 10–16. Available from: <https://doi.org/10.2307/1943155>
- Cove, D.J., Perroud, P.-F., Charron, A.J., McDaniel, S.F., Khandelwal, A. & Quatrano, R.S. (2009) The moss *Physcomitrella patens*: a novel model system for plant development and genomic studies. *Cold Spring Harbor Protocols*, **2009**(2), 115. Available from: <https://doi.org/10.1101/pdb.emo115>
- Davey, M.L., Tsuneda, A. & Currah, R.S. (2009) Pathogenesis of bryophyte hosts by the ascomycete *Atrididymella muscivora*. *American Journal of Botany*, **96**(7), 1274–1280. Available from: <https://doi.org/10.3732/ajb.0800239>
- de Vries, J. & Archibald, J.M. (2018) Plant evolution: landmarks on the path to terrestrial life. *New Phytologist*, **217**(4), 1428–1434. Available from: <https://doi.org/10.1111/nph.14975>
- Delaux, P.-M., Radhakrishnan, G.V., Jayaraman, D., Cheema, J., Malbreil, M., Volkening, J.D. *et al.* (2015) Algal ancestor of land plants was pre-adapted for symbiosis. *Proceedings of the National Academy of Sciences*, **112**(43), 13390–13395. Available from: <https://doi.org/10.1073/pnas.1515426112>
- Delaux, P.-M. & Schornack, S. (2021) Plant evolution driven by interactions with symbiotic and pathogenic microbes. *Science*, **371**(6531), 6605. Available from: <https://doi.org/10.1126/science.aba6605>
- Denancé, N., Szurek, B. & Noël, L.D. (2014) Emerging functions of nodulin-like proteins in non-nodulating plant species. *Plant and Cell Physiology*, **55**(3), 469–474. Available from: <https://doi.org/10.1093/pcp/pct198>
- Desirò, A., Hao, Z., Liber, J.A., Benucci, G.M.N., Lowry, D., Roberson, R. *et al.* (2018) Mycoplasma-related endobacteria within *Mortierella mycotina* fungi: diversity, distribution and functional insights into their lifestyle. *The ISME Journal*, **12**(7), 1743–1757. Available from: <https://doi.org/10.1038/s41396-018-0053-9>
- Dickie, I.A., Martínez-García, L.B., Koele, N., Grelet, G.-A., Tyljanakis, J.M., Peltzer, D.A. *et al.* (2013) Mycorrhizas and mycorrhizal fungal communities throughout ecosystem development. *Plant and Soil*, **367**(1), 11–39. Available from: <https://doi.org/10.1007/s11104-013-1609-0>
- Douglas, C.M. (2001) Fungal beta(1,3)-D-glucan synthesis. *Medical Mycology*, **39**(Suppl 1), 55–66. Available from: <https://doi.org/10.1080/mmy.39.1.55.66>
- Du, X., Yang, Z., Ariza, A.J.F., Wang, Q., Xie, G., Li, S. *et al.* (2022) Structure of plant RNA-DEPENDENT RNA POLYMERASE 2, an enzyme involved in small interfering RNA production. *The Plant Cell*, **34**(6), 2140–2149. Available from: <https://doi.org/10.1093/plcell/koac067>
- Du, Z.-Y., Zienkiewicz, K., Vande Pol, N., Ostrom, N.E., Benning, C. & Bonito, G.M. (2019) Algal-fungal symbiosis leads to photosynthetic mycelium. *eLife*, **8**, e47815. Available from: <https://doi.org/10.7554/eLife.47815>
- Duckett, J.G., Carafa, A. & Ligrone, R. (2006) A highly differentiated glomeromycete association with the mucilage-secreting, primitive antipodean

- liverwort *Treubia* (Treubiaceae): clues to the origins of mycorrhizas. *American Journal of Botany*, **93**(6), 797–813. Available from: <https://doi.org/10.3732/ajb.93.6.797>
- Eastburn, D.M., McElrone, A.J. & Bilgin, D.D. (2011) Influence of atmospheric and climatic change on plant–pathogen interactions. *Plant Pathology*, **60**(1), 54–69. Available from: <https://doi.org/10.1111/j.1365-3059.2010.02402.x>
- Feijen, F.A.A., Vos, R.A., Nuytinck, J. & Merckx, V.S.F.T. (2018) Evolutionary dynamics of mycorrhizal symbiosis in land plant diversification. *Scientific Reports*, **8**(1), 10698. Available from: <https://doi.org/10.1038/s41598-018-28920-x>
- Fonseca, H.M.A.C. & Barbara, R.L.L. (2008) Does *Lunularia cruciata* form symbiotic relationships with either *Glomus proliferum* or *G. intraradices*? *Mycological Research*, **112**(9), 1063–1068. Available from: <https://doi.org/10.1016/j.mycres.2008.03.008>
- Fontana, D.C., de Paula, S., Torres, A.G., de Souza, V.H.M., Pascholati, S.F., Schmidt, D. *et al.* (2021) Endophytic fungi: biological control and induced resistance to phytopathogens and abiotic stresses. *Pathogens*, **10**(5), 570. Available from: <https://doi.org/10.3390/pathogens10050570>
- Friesen, J.A. & Rodwell, V.W. (2004) The 3-hydroxy-3-methylglutaryl coenzyme-A (HMG-CoA) reductases. *Genome Biology*, **5**(11), 248. Available from: <https://doi.org/10.1186/gb-2004-5-11-248>
- Fürst-Jansen, J.M.R., de Vries, S. & de Vries, J. (2020) Evo-physio: on stress responses and the earliest land plants. *Journal of Experimental Botany*, **71**(11), 3254–3269. Available from: <https://doi.org/10.1093/jxb/eraa007>
- Gang, H., Li, R., Zhao, Y., Liu, G., Chen, S. & Jiang, J. (2019) Loss of GLK1 transcription factor function reveals new insights in chlorophyll biosynthesis and chloroplast development. *Journal of Experimental Botany*, **70**(12), 3125–3138. Available from: <https://doi.org/10.1093/jxb/erz128>
- Garcias-Morales, D., Palomar, V.M., Charlot, F., Nogué, F., Covarrubias, A.A. & Reyes, J.L. (2023) N6-methyladenosine modification of mRNA contributes to the transition from 2D to 3D growth in the moss *Physcomitrium patens*. *The Plant Journal*, **114**(1), 7–22. Available from: <https://doi.org/10.1111/tbj.16149>
- Gehan, M.A., Fahlgren, N., Abbasi, A., Berry, J.C., Callen, S.T., Chavez, L. *et al.* (2017) PlantCV v2: image analysis software for high-throughput plant phenotyping. *PeerJ*, **5**, e4088. Available from: <https://doi.org/10.7717/peerj.4088>
- Giauque, H. & Hawkes, C.V. (2013) Climate affects symbiotic fungal endophyte diversity and performance. *American Journal of Botany*, **100**(7), 1435–1444. Available from: <https://doi.org/10.3732/ajb.1200568>
- Goralgia, G.S., Liu, T.-K., Zhao, L., Panipinto, P.M., Groover, E.D., Bains, Y.S. *et al.* (2017) CYCLING DOF FACTOR 1 represses transcription through the TOPLESS co-repressor to control photoperiodic flowering in *Arabidopsis*. *The Plant Journal: For Cell and Molecular Biology*, **92**(2), 244–262. Available from: <https://doi.org/10.1111/tbj.13649>
- Grabherr, M.G., Haas, B.J., Yassour, M., Levin, J.Z., Thompson, D.A., Amit, I. *et al.* (2011) Full-length transcriptome assembly from RNA-seq data without a reference genome. *Nature Biotechnology*, **29**(7), 644–652. Available from: <https://doi.org/10.1038/nbt.1883>
- Grigoriev, I.V., Nikitin, R., Haridas, S., Kuo, A., Ohm, R., Otilar, R. *et al.* (2014) MycoCosm portal: gearing up for 1000 fungal genomes. *Nucleic Acids Research*, **42**(D1), D699–D704. Available from: <https://doi.org/10.1093/nar/gkt1183>
- Groenewald, E.G. & van der Westhuizen, A.J. (1997) Prostaglandins and related substances in plants. *Botanical Review*, **63**(3), 199–220.
- Guo, Y. & Narisawa, K. (2018) Fungus–bacterium symbionts promote plant health and performance. *Microbes and Environments*, **33**(3), 239–241. Available from: <https://doi.org/10.1264/jsme2.ME3303rh>
- Hachez, C., Laloux, T., Reinhardt, H., Cavez, D., Degand, H., Grefen, C. *et al.* (2014) *Arabidopsis* SNAREs SYP61 and SYP121 coordinate the trafficking of plasma membrane aquaporin PIP2;7 to modulate the cell membrane water permeability. *The Plant Cell*, **26**(7), 3132–3147. Available from: <https://doi.org/10.1105/tpc.114.127159>
- Hall, M.A., Kapuya, J.A., Sivakumaran, S. & John, A. (1977) The role of ethylene in the response of plants to stress. *Pesticide Science*, **8**(3), 217–223. Available from: <https://doi.org/10.1002/ps.2780080307>
- Hanke, S. & Rensing, S. (2010) In vitro association of non-seed plant gametophytes with arbuscular mycorrhiza fungi. *Endocytobiosis and Cell Research*, **20**, 95–101.
- Hayashi, K., Horie, K., Hiwatashi, Y., Kawaide, H., Yamaguchi, S., Hanada, A. *et al.* (2010) Endogenous diterpenes derived from ent-kaurene, a common gibberellin precursor, regulate protonema differentiation of the moss *Physcomitrella patens*. *Plant Physiology*, **153**(3), 1085–1097. Available from: <https://doi.org/10.1104/pp.110.157909>
- Hobbie, E.A. & Boyce, C.K. (2010) Carbon sources for the Palaeozoic giant fungus *Prototaxites* inferred from modern analogues. *Proceedings of the Royal Society B: Biological Sciences*, **277**(1691), 2149–2156. Available from: <https://doi.org/10.1098/rspb.2010.0201>
- Hu, Y., Zhong, S., Zhang, M., Liang, Y., Gong, G., Chang, X. *et al.* (2020) Potential role of photosynthesis in the regulation of reactive oxygen species and defence responses to *Blumeria graminis* f. sp. *tritici* in wheat. *International Journal of Molecular Sciences*, **21**(16), 16. Available from: <https://doi.org/10.3390/ijms21165767>
- Hunter, L.J.R., Westwood, J.H., Heath, G., Macaulay, K., Smith, A.G., MacFarlane, S.A. *et al.* (2013) Regulation of RNA-dependent RNA polymerase 1 and Isochorismate synthase gene expression in *Arabidopsis*. *PLoS One*, **8**(6), e66530. Available from: <https://doi.org/10.1371/journal.pone.0066530>
- Hutin, C., Nussaume, L., Moise, N., Moya, I., Kloppstech, K. & Havaux, M. (2003) Early light-induced proteins protect *Arabidopsis* from photooxidative stress. *Proceedings of the National Academy of Sciences of the United States of America*, **100**(8), 4921–4926. Available from: <https://doi.org/10.1073/pnas.0736939100>
- Ishida, T., Sugiyama, T., Tabei, N. & Yanagisawa, S. (2014) Diurnal expression of CONSTANS-like genes is independent of the function of cycling DOF factor (CDF)-like transcriptional repressors in *Physcomitrella patens*. *Plant Biotechnology*, **31**(4), 293–299. Available from: <https://doi.org/10.5511/plantbiotechnology.14.0821a>
- Ivarsson, M., Drake, H., Bengtson, S. & Rasmussen, B. (2020) A cryptic alternative for the evolution of hyphae. *BioEssays*, **42**(6), 1900183. Available from: <https://doi.org/10.1002/bies.201900183>
- Ivashuta, S., Liu, J., Liu, J., Lohar, D.P., Haridas, S., Bucciarelli, B. *et al.* (2005) RNA interference identifies a calcium-dependent protein kinase involved in *Medicago truncatula* root development. *The Plant Cell*, **17**(11), 2911–2921. Available from: <https://doi.org/10.1105/tpc.105.035394>
- Jermy, A. (2011) Soil fungi helped ancient plants to make land. *Nature Reviews Microbiology*, **9**(1), 2494. Available from: <https://doi.org/10.1038/nrmicro2494>
- Johnson, J.M., Ludwig, A., Furch, A.C.U., Mithöfer, A., Scholz, S., Reichelt, M. *et al.* (2019) The beneficial root-colonizing fungus *Mortierella hyalina* promotes the aerial growth of *Arabidopsis* and activates calcium-dependent responses that restrict *Alternaria brassicae*-induced disease development in roots. *Molecular Plant–Microbe Interactions*, **32**(3), 351–363. Available from: <https://doi.org/10.1094/MPMI-05-18-0115-R>
- Kluyver, T., Ragan-Kelley, B., Pérez, F., Granger, B., Bussonnier, M., Frederic, J. *et al.* (2016) Jupyter Notebooks – a publishing format for reproducible computational workflows. In: Loizides, F. & Schmidt, B. (Eds.) *Positioning and power in academic publishing: players, agents and agendas*. Amsterdam: IOS Press, pp. 87–90. Available from: <https://doi.org/10.3233/978-1-61499-649-1-87>
- Knack, J.J., Wilcox, L.W., Delaux, P.-M., Ané, J.-M., Piotrowski, M.J., Cook, M.E. *et al.* (2015) Microbiomes of streptophyte algae and bryophytes suggest that a functional suite of microbiota fostered plant colonization of land. *International Journal of Plant Sciences*, **176**(5), 405–420. Available from: <https://doi.org/10.1086/681161>
- Kohler, A., Kuo, A., Nagy, L.G., Morin, E., Barry, K.W., Buscot, F. *et al.* (2015) Convergent losses of decay mechanisms and rapid turnover of symbiosis genes in mycorrhizal mutualists. *Nature Genetics*, **47**(4), 410–415. Available from: <https://doi.org/10.1038/ng.3223>
- Kolosova, N., Miller, B., Ralph, S., Ellis, B.E., Douglas, C., Ritland, K. *et al.* (2004) Isolation of high-quality RNA from gymnosperm and angiosperm trees. *BioTechniques*, **36**(5), 821–824. Available from: <https://doi.org/10.2144/04365ST06>
- Lam, K.-K., LaButti, K., Khalak, A. & Tse, D. (2015) FinisherSC: a repeat-aware tool for upgrading de novo assembly using long reads. *Bioinformatics*, **31**(19), 3207–3209. Available from: <https://doi.org/10.1093/bioinformatics/btv280>
- Lang, D., Ullrich, K.K., Murat, F., Fuchs, J., Jenkins, J., Haas, F.B. *et al.* (2018) The *Physcomitrella patens* chromosome-scale assembly reveals moss genome structure and evolution. *The Plant Journal*, **93**(3), 515–533. Available from: <https://doi.org/10.1111/tbj.13801>

- Lehtonen, M.T., Akita, M., Kalkkinen, N., Ahola-livarinen, E., Rönholm, G., Somervuo, P. *et al.* (2009) Quickly-released peroxidase of moss in defense against fungal invaders. *New Phytologist*, **183**(2), 432–443. Available from: <https://doi.org/10.1111/j.1469-8137.2009.02864.x>
- Lehtonen, M.T., Martinen, E.M., Akita, M. & Valkonen, J.P.T. (2012) Fungi infecting cultivated moss can also cause diseases in crop plants. *Annals of Applied Biology*, **160**(3), 298–307. Available from: <https://doi.org/10.1111/j.1744-7348.2012.00543.x>
- Li, F., Cheng, C., Cui, F., de Oliveira, M.V.V., Yu, X., Meng, X. *et al.* (2014) Modulation of RNA polymerase II phosphorylation downstream of pathogen perception orchestrates plant immunity. *Cell Host & Microbe*, **16**(6), 748–758. Available from: <https://doi.org/10.1016/j.chom.2014.10.018>
- Liao, H.-L. (2021) The plant-growth-promoting fungus, *Mortierella elongata*: its biology, ecological distribution, and growth-promoting activities: SS679/SL466, 3/2021. *EDIS*, **2021**(2), 2. Available from: <https://doi.org/10.32473/edis-ss679-2021>
- Licausi, F., Ohme-Takagi, M. & Perata, P. (2013) APETALA2/ethylene responsive factor (AP2/ERF) transcription factors: mediators of stress responses and developmental programs. *New Phytologist*, **199**(3), 639–649. Available from: <https://doi.org/10.1111/nph.12291>
- Liepiņa, L. (2012) Occurrence of fungal structures in bryophytes of the boreo-northern zone. *Environmental and Experimental Biology*, **10**, 35–40.
- Ligrone, R., Carafa, A., Lumini, E., Bianciotto, V., Bonfante, P. & Duckett, J.G. (2007) Glomeromycotan associations in liverworts: a molecular, cellular, and taxonomic analysis. *American Journal of Botany*, **94**(11), 1756–1777. Available from: <https://doi.org/10.3732/ajb.94.11.1756>
- Loron, C.C., François, C., Rainbird, R.H., Turner, E.C., Borensztajn, S. & Javaux, E.J. (2019) Early fungi from the Proterozoic era in Arctic Canada. *Nature*, **570**, 232–235. Available from: <https://doi.org/10.1038/s41586-019-1217-0>
- Love, M.I., Huber, W. & Anders, S. (2014) Moderated estimation of fold change and dispersion for RNA-seq data with DESeq2. *Genome Biology*, **15**(12), 550. Available from: <https://doi.org/10.1186/s13059-014-0550-8>
- Lu, Y. & Yao, J. (2018) Chloroplasts at the crossroad of photosynthesis, pathogen infection and plant defense. *International Journal of Molecular Sciences*, **19**, 3900. Available from: <https://doi.org/10.3390/ijms19123900>
- Lutzoni, F., Nowak, M.D., Alfaro, M.E., Reeb, V., Miadlikowska, J., Krug, M. *et al.* (2018) Contemporaneous radiations of fungi and plants linked to symbiosis. *Nature Communications*, **9**(1), 5451. Available from: <https://doi.org/10.1038/s41467-018-07849-9>
- Lutzoni, F., Pagel, M. & Reeb, V. (2001) Major fungal lineages are derived from lichen symbiotic ancestors. *Nature*, **411**(6840), 937–940. Available from: <https://doi.org/10.1038/35082053>
- Machado, L., Castro, A., Hamberg, M., Bannenberg, G., Gaggero, C., Castresana, C. *et al.* (2015) The *Physcomitrella patens* unique alpha-dioxygenase participates in both developmental processes and defense responses. *BMC Plant Biology*, **15**(1), 45. Available from: <https://doi.org/10.1186/s12870-015-0439-z>
- Mariconti, L., Pellegrini, B., Cantoni, R., Stevens, R., Bergounioux, C., Cella, R. *et al.* (2002) THE E2F family of transcription factors from *Arabidopsis thaliana*: novel and conserved components of the retinoblastoma/E2F pathway in plants. *Journal of Biological Chemistry*, **277**(12), 9911–9919. Available from: <https://doi.org/10.1074/jbc.M110616200>
- Martin, F. & Nehls, U. (2009) Harnessing ectomycorrhizal genomics for ecological insights. *Current Opinion in Plant Biology*, **12**(4), 508–515. Available from: <https://doi.org/10.1016/j.pbi.2009.05.007>
- Maughan, S.C., Pasternak, M., Cairns, N., Kiddle, G., Brach, T., Jarvis, R. *et al.* (2010) Plant homologs of the *Plasmodium falciparum* chloroquine-resistance transporter, PfCRT, are required for glutathione homeostasis and stress responses. *Proceedings of the National Academy of Sciences of the United States of America*, **107**(5), 2331–2336. Available from: <https://doi.org/10.1073/pnas.0913689107>
- Mittag, J., Sola, I., Rusak, G. & Ludwig-Müller, J. (2015) *Physcomitrella patens* auxin conjugate synthetase (GH3) double knockout mutants are more resistant to *Pythium* infection than wild type. *Journal of Plant Physiology*, **183**, 75–83. Available from: <https://doi.org/10.1016/j.jplph.2015.05.015>
- Miyazaki, S., Hara, M., Ito, S., Tanaka, K., Asami, T., Hayashi, K. *et al.* (2018) An ancestral gibberellin in a moss *Physcomitrella patens*. *Molecular Plant*, **11**(8), 1097–1100. Available from: <https://doi.org/10.1016/j.molp.2018.03.010>
- Miyazaki, S., Katsumata, T., Natsume, M. & Kawaide, H. (2011) The CYP701B1 of *Physcomitrella patens* is an ent-kaurene oxidase that resists inhibition by uniconazole-P. *FEBS Letters*, **585**(12), 1879–1883. Available from: <https://doi.org/10.1016/j.febslet.2011.04.057>
- Modi, A., Vai, S., Caramelli, D. & Lari, M. (2021) The Illumina sequencing protocol and the NovaSeq 6000 system. In: Mengoni, A., Bacci, G. & Fondi, M. (Eds.) *Bacterial pangenomics: methods and protocols*. US: Springer, pp. 15–42. Available from: https://doi.org/10.1007/978-1-0716-1099-2_2
- Morikawa, T., Saga, H., Hashizume, H. & Ohta, D. (2009) CYP710A genes encoding sterol C22-desaturase in *Physcomitrella patens* as molecular evidence for the evolutionary conservation of a sterol biosynthetic pathway in plants. *Planta*, **229**(6), 1311–1322. Available from: <https://doi.org/10.1007/s00425-009-0916-4>
- Morris, J.L., Puttick, M.N., Clark, J.W., Edwards, D., Kenrick, P., Pressel, S. *et al.* (2018) The timescale of early land plant evolution. *Proceedings of the National Academy of Sciences of the United States of America*, **115**(10), E2274–E2283. Available from: <https://doi.org/10.1073/pnas.1719588115>
- Mueller, M.J. (1998) Radically novel prostaglandins in animals and plants: the isoprostanes. *Chemistry & Biology*, **5**(12), R323–R333. Available from: [https://doi.org/10.1016/S1074-5521\(98\)90660-3](https://doi.org/10.1016/S1074-5521(98)90660-3)
- Müller, H., Bracken, A.P., Vernell, R., Moroni, M.C., Christians, F., Grassilli, E. *et al.* (2001) E2Fs regulate the expression of genes involved in differentiation, development, proliferation, and apoptosis. *Genes & Development*, **15**(3), 267–285. Available from: <https://doi.org/10.1101/gad.864201>
- Nakano, Y., Yamaguchi, M., Endo, H., Rejab, N.A. & Ohtani, M. (2015) NAC-MYB-based transcriptional regulation of secondary cell wall biosynthesis in land plants. *Frontiers in Plant Science*, **6**, 288. Available from: <https://doi.org/10.3389/fpls.2015.00288>
- Naumann, M., Schübler, A. & Bonfante, P. (2010) The obligate endobacteria of arbuscular mycorrhizal fungi are ancient heritable components related to the mollicutes. *The ISME Journal*, **4**, 862–871. Available from: <https://doi.org/10.1038/ismej.2010.21>
- Nelsen, M.P., Lücking, R., Boyce, C.K., Lumbsch, H.T. & Ree, R.H. (2020) No support for the emergence of lichens prior to the evolution of vascular plants. *Geobiology*, **18**(1), 3–13. Available from: <https://doi.org/10.1111/gbi.12369>
- Nguyen, T.T.T., Park, S.W., Pangging, M. & Lee, H.B. (2019) Molecular and morphological confirmation of three undescribed species of *Mortierella* from Korea. *Mycobiology*, **47**(1), 31–39. Available from: <https://doi.org/10.1080/12298093.2018.1551854>
- Oshima, S., Sato, Y., Fujimura, R., Takashima, Y., Hamada, M., Nishizawa, T. *et al.* (2016) *Mycovoidus cysteinexigens* gen. nov., sp. nov., an endohyphal bacterium isolated from a soil isolate of the fungus *Mortierella elongata*. *International Journal of Systematic and Evolutionary Microbiology*, **66**(5), 2052–2057. Available from: <https://doi.org/10.1099/ijsem.0.000990>
- Otero-Blanca, A., Pérez-Llano, Y., Reboledo-Blanco, G., Lira-Ruan, V., Padilla-Chacon, D., Folch-Mallol, J.L. *et al.* (2021) *Physcomitrium patens* infection by *Colletotrichum gloeosporioides*: understanding the fungal-bryophyte interaction by microscopy, phenomics and RNA sequencing. *Journal of Fungi*, **7**(8), 677. Available from: <https://doi.org/10.3390/jof7080677>
- Patro, R., Duggal, G., Love, M.I., Irizarry, R.A. & Kingsford, C. (2017) Salmon: fast and bias-aware quantification of transcript expression using dual-phase inference. *Nature Methods*, **14**(4), 417–419. Available from: <https://doi.org/10.1038/nmeth.4197>
- Perroud, P.-F., Haas, F.B., Hiss, M., Ullrich, K.K., Alboresi, A., Amirebrahimi, M. *et al.* (2018) The *Physcomitrella patens* gene atlas project: large-scale RNA-seq based expression data. *The Plant Journal*, **95**(1), 168–182. Available from: <https://doi.org/10.1111/tpj.13940>
- Ponce de León, I. (2011) The Moss *Physcomitrella patens* as a model system to study interactions between plants and phytopathogenic fungi and oomycetes. *Journal of Pathogens*, **2011**, e719873. Available from: <https://doi.org/10.4061/2011/719873>
- Ponce De León, I., Schmelz, E.A., Gaggero, C., Castro, A., Álvarez, A. & Montesano, M. (2012) *Physcomitrella patens* activates reinforcement of the cell wall, programmed cell death and accumulation of evolutionary conserved defence signals, such as salicylic acid and 12-oxo-phytodienoic acid, but not jasmonic acid, upon *Botrytis cinerea* infection.

- Molecular Plant Pathology*, 13(8), 960–974. Available from: <https://doi.org/10.1111/j.1364-3703.2012.00806.x>
- Proust, H., Hoffmann, B., Xie, X., Yoneyama, K., Schaefer, D.G., Yoneyama, K. *et al.* (2011) Strigolactones regulate protonema branching and act as a quorum sensing-like signal in the moss *Physcomitrella patens*. *Development*, 138(8), 1531–1539. Available from: <https://doi.org/10.1242/dev.058495>
- Rathgeb, U., Chen, M., Buron, F., Feddermann, N., Schorderet, M., Raisin, A. *et al.* (2020) VAPYRIN-like is required for development of the moss *Physcomitrella patens*. *Development*, 147(11), 762. Available from: <https://doi.org/10.1242/dev.184762>
- Raudvere, U., Kolberg, L., Kuzmin, I., Arak, T., Adler, P., Peterson, H. *et al.* (2019) G:profiler: a web server for functional enrichment analysis and conversions of gene lists (2019 update). *Nucleic Acids Research*, 47(W1), W191–W198. Available from: <https://doi.org/10.1093/nar/gkz369>
- Read, D.J., Duckett, J.G., Francis, R., Ligrone, R. & Russell, A. (2000) Symbiotic fungal associations in “lower” land plants. *Philosophical Transactions of the Royal Society of London. Series B, Biological Sciences*, 355, 815–831. Available from: <https://doi.org/10.1098/rstb.2000.0617>
- Reboledo, G., Agorio, A.D., Vignale, L., Batista-García, R.A. & Ponce De León, I. (2021) Transcriptional profiling reveals conserved and species-specific plant defense responses during the interaction of *Physcomitrium patens* with *Botrytis cinerea*. *Plant Molecular Biology*, 107(4), 365–385. Available from: <https://doi.org/10.1007/s11103-021-01116-0>
- Reboledo, G., Agorio, A., Vignale, L., Batista-García, R.A. & Ponce De León, I. (2020) *Botrytis cinerea* transcriptome during the infection process of the bryophyte *Physcomitrium patens* and angiosperms. *Journal of Fungi*, 7(1), 11. Available from: <https://doi.org/10.3390/jof7010011>
- Reimand, J., Kull, M., Peterson, H., Hansen, J. & Vilo, J. (2007) G:profiler—a web-based toolset for functional profiling of gene lists from large-scale experiments. *Nucleic Acids Research*, 35, W193–W200. Available from: <https://doi.org/10.1093/nar/gkm226>
- Rensing, S.A., Lang, D., Zimmer, A.D., Terry, A., Salamov, A., Shapiro, H. *et al.* (2008) The *Physcomitrella* genome reveals evolutionary insights into the conquest of land by plants. *Science*, 319(5859), 64–69. Available from: <https://doi.org/10.1126/science.1150646>
- Reski, R. & Abel, W.O. (1985) Induction of budding on chloronemata and caulonemata of the moss, *Physcomitrella patens*, using isopentenyladenine. *Planta*, 165(3), 354–358. Available from: <https://doi.org/10.1007/BF00392232>
- Roberts, A., Roberts, E. & Haigler, C. (2012) Moss cell walls: structure and biosynthesis. *Frontiers in Plant Science*, 3, 166. Available from: <https://doi.org/10.3389/fpls.2012.00166>
- Roberts, A.W., Lahnstein, J., Hsieh, Y.S.Y., Xing, X., Yap, K., Chaves, A.M. *et al.* (2018) Functional characterization of a glycosyltransferase from the moss *Physcomitrella patens* involved in the biosynthesis of a novel cell wall arabinoglucan. *The Plant Cell*, 30(6), 1293–1308. Available from: <https://doi.org/10.1105/tpc.18.00082>
- Russell, J. & Bulman, S. (2005) The liverwort *Marchantia foliacea* forms a specialized symbiosis with arbuscular mycorrhizal fungi in the genus *glomus*. *New Phytologist*, 165(2), 567–579. Available from: <https://doi.org/10.1111/j.1469-8137.2004.01251.x>
- Salvioli, A., Ghignone, S., Novero, M., Navazio, L., Venice, F., Bagnaresi, P. *et al.* (2016) Symbiosis with an endobacterium increases the fitness of a mycorrhizal fungus, raising its bioenergetic potential. *The ISME Journal*, 10(1), 130–144. Available from: <https://doi.org/10.1038/ismej.2015.91>
- Savage, Z., Duggan, C., Toufexi, A., Pandey, P., Liang, Y., Segretin, M.E. *et al.* (2021) Chloroplasts alter their morphology and accumulate at the pathogen interface during infection by *Phytophthora infestans*. *The Plant Journal*, 107(6), 1771–1787. Available from: <https://doi.org/10.1111/tj.15416>
- Scharte, J., Schön, H. & Weis, E. (2005) Photosynthesis and carbohydrate metabolism in tobacco leaves during an incompatible interaction with *Phytophthora nicotianae*. *Plant, Cell & Environment*, 28(11), 1421–1435. Available from: <https://doi.org/10.1111/j.1365-3040.2005.01380.x>
- Simkin, A.J., Guirimand, G., Papon, N., Courdavault, V., Thabet, I., Ginis, O. *et al.* (2011) Peroxisomal localisation of the final steps of the mevalonic acid pathway in planta. *Planta*, 234(5), 903–914. Available from: <https://doi.org/10.1007/s00425-011-1444-6>
- Smith, S.E. & Read, D.J. (2010) *Mycorrhizal symbiosis*. London: Academic Press.
- Soneson, C., Love, M.I. & Robinson, M.D. (2016) Differential analyses for RNA-seq: transcript-level estimates improve gene-level inferences. *F1000Research*, 4, 1521. Available from: <https://doi.org/10.12688/f1000research.7563.2>
- Soufi, A. & Jayaraman, P.-S. (2008) PRH/hex: an oligomeric transcription factor and multifunctional regulator of cell fate. *The Biochemical Journal*, 412(3), 399–413. Available from: <https://doi.org/10.1042/BJ20080035>
- Stenzel, I., Hause, B., Miersch, O., Kurz, T., Maucher, H., Weichert, H. *et al.* (2003) Jasmonate biosynthesis and the allene oxide cyclase family of *Arabidopsis thaliana*. *Plant Molecular Biology*, 51(6), 895–911. Available from: <https://doi.org/10.1023/A:1023049319723>
- Su, C. (2023) Pectin modifications at the symbiotic interface. *New Phytologist*, 238(1), 25–32. Available from: <https://doi.org/10.1111/nph.18705>
- Swarbrick, P.J., Schulze-Lefert, P. & Scholes, J.D. (2006) Metabolic consequences of susceptibility and resistance (race-specific and broad-spectrum) in barley leaves challenged with powdery mildew. *Plant, Cell & Environment*, 29(6), 1061–1076. Available from: <https://doi.org/10.1111/j.1365-3040.2005.01472.x>
- Takahashi, T. & Kakehi, J.-I. (2010) Polyamines: ubiquitous polyocations with unique roles in growth and stress responses. *Annals of Botany*, 105(1), 1–6. Available from: <https://doi.org/10.1093/aob/mcp259>
- Tominaga, M., Kojima, H., Yokota, E., Nakamori, R., Anson, M., Shimmen, T. *et al.* (2012) Calcium-induced mechanical change in the neck domain alters the activity of plant myosin XI. *The Journal of Biological Chemistry*, 287(36), 30711–30718. Available from: <https://doi.org/10.1074/jbc.M112.346668>
- Uehling, J., Gryganskyi, A., Hameed, K., Tschaplinski, T., Misztal, P.K., Wu, S. *et al.* (2017) Comparative genomics of *Mortierella elongata* and its bacterial endosymbiont *Mycosporium cysteinexigens*. *Environmental Microbiology*, 19(8), 2964–2983. Available from: <https://doi.org/10.1111/1462-2920.13669>
- Vandepol, N., Liber, J., Yocca, A., Matlock, J., Edger, P. & Bonito, G. (2022) *Linum catharticum* (Mortierellaceae) stimulates *Arabidopsis thaliana* aerial growth and responses to auxin, ethylene, and reactive oxygen species. *PLoS One*, 17(4), e0261908. Available from: <https://doi.org/10.1371/journal.pone.0261908>
- Vega-Sánchez, M.E., Verherbruggen, Y., Scheller, H.V. & Ronald, P.C. (2013) Abundance of mixed linkage glucan in mature tissues and secondary cell walls of grasses. *Plant Signaling & Behavior*, 8(2), e23143. Available from: <https://doi.org/10.4161/psb.23143>
- Verma, A., Shameem, N., Jatav, H.S., Sathyanarayana, E., Parray, J.A., Poczai, P. *et al.* (2022) Fungal endophytes to combat biotic and abiotic stresses for climate-smart and sustainable agriculture. *Frontiers in Plant Science*, 13, 953836. Available from: <https://doi.org/10.3389/fpls.2022.953836>
- Voiniciuc, C., Pauly, M. & Usadel, B. (2018) Monitoring polysaccharide dynamics in the plant cell wall. *Plant Physiology*, 176(4), 2590–2600. Available from: <https://doi.org/10.1104/pp.17.01776>
- Waller, K.L., Muhle, R.A., Ursos, L.M., Horrocks, P., Verdier-Pinard, D., Sidhu, A.B.S. *et al.* (2003) Chloroquine resistance modulated *in vitro* by expression levels of the *Plasmodium falciparum* chloroquine resistance transporter. *Journal of Biological Chemistry*, 278(35), 33593–33601. Available from: <https://doi.org/10.1074/jbc.M302215200>
- Wang, J., Lian, N., Zhang, Y., Man, Y., Chen, L., Yang, H. *et al.* (2022) The cytoskeleton in plant immunity: dynamics, regulation, and function. *International Journal of Molecular Sciences*, 23, 553. Available from: <https://doi.org/10.3390/ijms232415553>
- Wang, X. & He, Y. (2015) Tissue culturing and harvesting of Protonemata from the Moss *Physcomitrella patens*. *Bio-Protocol*, 5(15), 1556. Available from: <https://doi.org/10.21769/BioProtoc.1556>
- Waters, M.T., Scaffidi, A., Flematti, G.R. & Smith, S.M. (2013) The origins and mechanisms of karrikin signalling. *Current Opinion in Plant Biology*, 16(5), 667–673. Available from: <https://doi.org/10.1016/j.pbi.2013.07.005>
- Waters, M.T., Wang, P., Korkaric, M., Capper, R.G., Saunders, N.J. & Langdale, J.A. (2009) GLK transcription factors coordinate expression of the photosynthetic apparatus in *Arabidopsis*. *The Plant Cell*, 21(4), 1109–1128. Available from: <https://doi.org/10.1105/tpc.108.065250>
- Wei, Q., Wang, W., Hu, T., Hu, H., Mao, W., Zhu, Q. *et al.* (2018) Genome-wide identification and characterization of Dof transcription factors in eggplant (*Solanum melongena* L.). *PeerJ*, 6, e4481. Available from: <https://doi.org/10.7717/peerj.4481>

- White, J.F., Jr. & Torres, M.S.** (2010) Is plant endophyte-mediated defensive mutualism the result of oxidative stress protection? *Physiologia Plantarum*, **138**(4), 440–446. Available from: <https://doi.org/10.1111/j.1399-3054.2009.01332.x>
- Xia, W., Yu, H., Cao, P., Luo, J. & Wang, N.** (2017) Identification of TIFY family genes and analysis of their expression profiles in response to phytohormone treatments and *Melampsora larici-populina* infection in poplar. *Frontiers in Plant Science*, **8**, 493. Available from: <https://doi.org/10.3389/fpls.2017.00493>
- Yang, Z., Duan, L., Li, H., Tang, T., Chen, L., Hu, K. et al.** (2022) Regulation of heat stress in *Physcomitrium* (*Physcomitrella*) *patens* provides novel insight into the functions of plant RNase H1s. *International Journal of Molecular Sciences*, **23**(16), 270. Available from: <https://doi.org/10.3390/ijms23169270>
- Yasumura, Y., Moylan, E.C. & Langdale, J.A.** (2005) A conserved transcription factor mediates nuclear control of organelle biogenesis in anciently diverged land plants. *The Plant Cell*, **17**(7), 1894–1907. Available from: <https://doi.org/10.1105/tpc.105.033191>
- Yin, Y., Vafeados, D., Tao, Y., Yoshida, S., Asami, T. & Chory, J.** (2005) A new class of transcription factors mediates Brassinosteroid-regulated gene expression in Arabidopsis. *Cell*, **120**(2), 249–259. Available from: <https://doi.org/10.1016/j.cell.2004.11.044>
- Zhang, K., Bonito, G., Hsu, C.-M., Hameed, K., Vilgalys, R. & Liao, H.-L.** (2020) *Mortierella elongata* increases plant biomass among non-leguminous crop species. *Agronomy*, **10**(5), 754. Available from: <https://doi.org/10.3390/agronomy10050754>
- Zhao, S., Ye, Z. & Stanton, R.** (2020) Misuse of RPKM or TPM normalization when comparing across samples and sequencing protocols. *RNA*, **26**, 903–909. Available from: <https://doi.org/10.1261/rna.074922.120>